UNIVERSITAT POLITÈCNICA DE VALÈNCIA

Escola Tècnica Superior d'Enginyeria Agronòmica i del Medi Natural

UNIVERSITAT POLITÈCNICA DE VALÈNCIA

Escuela Técnica Superior de Ingeniería Agronómica y del Medio Natural

Caracterización de efectores de la activación sinérgica de AMPK con metformina y salicilato que reducen la toxicidad producida por poliglutaminas en C. elegans.

Trabajo Fin de Grado

Grado en Biotecnología

AUTOR/A: Martínez Almudéver, Carmen

Tutor/a: Murguía Ibáñez, José Ramón

Cotutor/a externo: DEL VALLE CARRANZA, ANDREA

Director/a Experimental: TRUJILLO DEL RIO, CRISTINA

CURSO ACADÉMICO: 2022/2023

Characterization of downstream effectors of synergistic activation of AMPK with metformin and salicylate which reduce polyQ toxicity in *C. elegans.*

Bachelor's thesis
Bachelor's degree in biotechnology
Academic year 2022/2023
Universitat Politècnica de València
Escola Tècnica Superior d'Enginyeria Agronòmica i del Medi Natural

Author: Carmen Martínez Almudéver
Academic tutor: José Ramón Murguía Ibáñez
Experimental director: Andrea del Valle Carranza
Experimental codirector: Cristina Trujillo del Río

València, June 2023

TITLE: Characterization of downstream effectors of synergistic activation of AMPK with metformin and salicylate which reduce polyQ toxicity in *C. elegans.*

ABSTRACT: The diseases induced by polyglutamine expansions (polyQ) are a group of neurodegenerative disorders caused by expanded CAG repeats encoding a long polyQ tract in the respective proteins. Huntington disease (HD) is the most prevalent one and it is a rare autosomal dominant neurodegenerative disorder characterized by progressive motor and cognitive impairments. It is caused by an abnormal expansion of CAG triplets in the huntingtin gene's (*HTT*) first exon, causing protein aggregation and toxicity.

No therapy has yet been proven effective, but some compounds, such as metformin, have been reported as potentially beneficial disease-modifiers of this pathology in animal models. Previous findings in the lab have shown that the synergistic activation of AMP-activated protein kinase (AMPK), with metformin and salicylate, reduces aggregation and neuronal damage in *C. elegans* models of toxicity induced by polyQs. AMPK is a master regulator of healthspan and lifespan modulating energy metabolism, stress resistance and cellular proteostasis. Nevertheless, it remains unclear whether this alleviation is dependent exclusively on AMPK, or other signalling pathways are implicated, since both drugs act pleiotropically.

This study validated the AMPK-dependent rescue by metformin and salicylate in solid media, which reflects more accurately the synergic effect. It was suggested that the treatment activates autophagy through LGG-1 to promote protein clearance and reduction of polyQ aggregates. Moreover, the necessity of functional AMPK to activate autophagy was demonstrated.

Nevertheless, the study of AMPK downstream effectors (HLH-30, SKN-1 and DAF-16) revealed their subcellular localization to be cytoplasmatic after synergic treatment. Therefore, given the collected data, it cannot be affirmed that these effectors do not participate in the response triggered by metformin and salicylate. Finally, RNA interference was used as a gene silencing tool to study the possible role the AMPK target DAF-16 in the protection against polyQ toxicity induced by metformin and salicylate. However, the obtained results are not conclusive since the control did not work.

This work is related to the SDG3 "Good health and well-being" from the 2023 Agenda.

KEYWORDS: *C. elegans*, AMPK, autophagy, polyQ, metformin, salicylate.

AUTHOR: Carmen Martínez Almudéver

DIRECTOR: Andrea del Valle Carranza

CODIRECTOR: Cristina Trujillo del Río

TUTOR: José Ramón Murguía Ibáñez

PLACE AND DATE: València, June 2023

TÍTULO: Caracterización de efectores de la activación sinérgica de AMPK con metformina y salicilato que reducen la toxicidad producida por poliglutaminas en *C. elegans.*

RESUMEN: Las enfermedades asociadas a expansiones de poliglutamina (poliQ) son un grupo de trastornos neurodegenerativos causados por repeticiones expandidas de CAG que codifican una larga cadena de poliQs en las proteínas respectivas. La enfermedad de Huntington (EH) es la más prevalente y es un trastorno neurodegenerativo autosómico dominante raro caracterizado por deterioro motor y cognitivo progresivo. Es causada por una expansión anormal de tripletes CAG en el primer exón del gen huntingtina (*HTT*), lo que provoca agregación y toxicidad de la proteína.

Hasta ahora no se ha demostrado que ninguna terapia sea efectiva, pero se ha observado que algunos compuestos, como la metformina, pueden ser beneficiosos en modelos animales de la enfermedad. Hallazgos previos en el laboratorio han mostrado que la activación sinérgica de la proteína quinasa activada por AMP (AMPK), con metformina y salicilato, reduce la agregación y el daño neuronal en modelos de toxicidad inducida por poliQs en *C. elegans*. AMPK es un regulador clave de la longevidad y la salud, modulando el metabolismo energético, la resistencia al estrés y la proteostasis celular. Sin embargo, aún no está claro si esta mejora depende exclusivamente de AMPK, o si otras vías de señalización están implicadas, ya que ambos fármacos actúan pleiotrópicamente.

Este estudio validó el rescate dependiente de AMPK por el efecto de la metformina y el salicilato en medio sólido, el cual refleja de manera más precisa el efecto sinérgico. Se sugirió que el tratamiento activa la autofagia a través de LGG-1 para promover la eliminación de proteínas y la reducción de agregados de poliglutaminas. Además, se demostró la necesidad de AMPK funcional para poder activar la autofagia.

Sin embargo, el estudio de los efectores aguas abajo de la AMPK (HLH-30, SKN-1 y DAF-16) reveló que su localización subcelular era citoplasmática después del tratamiento sinérgico. Por lo tanto, dados los datos recopilados, no se puede afirmar que estos efectores no participen en la respuesta desencadenada por la metformina y el salicilato. Por último, se utilizó la interferencia de ARN como herramienta para silenciar *daf-16* y estudiar su posible papel en la protección contra la toxicidad por poliglutaminas inducida por metformina y salicilato. Sin embargo, los resultados obtenidos no son concluyentes debido a que el control no funcionó.

Este trabajo se relaciona con los el ODS3 “Salud y bienestar” de la agenda 2023.

PALABRAS CLAVE: *C. elegans*, AMPK, autofagia, poliQ, metformina, salicilato.

AUTOR: Carmen Martínez Almudéver

DIRECTORA: Andrea del Valle Carranza

CODIRECTORA: Cristina Trujillo del Río

TUTOR: José Ramón Murguía Ibáñez

LUGAR Y FECHA: València, junio de 2023

AGRADECIMIENTOS

En primer lugar, agradecerle a Rafa abrirme las puertas de su laboratorio y enseñarme a los bichitos. Gracias por la confianza y por estar dispuesto a ayudar hasta desde la distancia.

Agradecer a Cris y Andu, las directoras de este trabajo, por todo lo que me han enseñado, por haber estado para lo que necesitara y sobre todo por la paciencia. En especial a Cris por guiarme cada día y ayudarme tantísimo.

Gracias a ellas y todas las chicas del lab: Julia, Lidón, Cinta, Belén, Pilar, Alba y Anapi. Por los consejos, por inspirarme y por hacerlo todo más ameno y mucho más divertido. Y un *acerdimiento* especial a Data.

Gracias a los amigos que me ha dado la carrera y me han acompañado estos cuatro largos años: Adri, Cris, Miguel, Juanto, María y Capi. No solo espero, sino sé que acabarán haciendo grandes cosas en el futuro.

Finalmente, gracias infinitas a mi familia por apoyarme siempre, por preguntarme y tener curiosidad por lo que hago, incluso cuando ni siquiera consiguen entender del todo lo que les explico.

TABLE OF CONTENTS

LIST OF FIGURES

LIST OF TABLES

ABREVIATIONS

40Q: 40 glutamines
AMP: Adenosine monophosphate
AMPK: Adenosine monophosphate kinase
ANOVA: analysis of variance
ATG: Autophagy-related
ATP: Adenosine triphosphate
***C. elegans*:** Caenorhabditis elegans
CACNA1 P: Calcium voltage-gated channel subunit alpha1 A
CAG: Cytosine-adenine-guanine triplet coding for glutamine
CRISPR : Clustered Regularly Interspaced Short Palindromic Repeats
DNA: Deoxyribonucleic acid
DRPLA: Dentatorubral-pallidoluysian atrophy
E. coli: Escherichia coli
E.V.: empty vector
FoxO: Forkhead Box O1
Gadd45a: Growth arrest and DNA-damage-inducible protein GADD45 alpha
GFP: Green fluorescent protein
Glu: Glutamine
gst-4: Glutathione S-transferase A4
HD: Huntington's disease
HLH-30: Helix-loop-helix protein 30
Htt: Huntingtin protein
HTT: Huntingtin gene
IGF-2: Insulin like growth factor 2
IIS: insulin/IGF-1 signaling
IPTG: Isopropyl β- d-1-thiogalactopyranoside
L*: larva stage 1,2,3 or 4
LB: Lysogenia Broth
LC3: Microtubule-associated protein 1A/1B-light chain 3
mHtt: Mutant huntingtin
mTOR: Mammalian target of rapamycin
NGM: Nematode growing media
Nrf2: Nuclear factor erythroid 2-related factor 2
PCR: Polymerase chain reaction
pmp-3: plasma membrane proteolipd 3
polyQ: Polyglutamine
RNA: Ribonucleic acid
RNAi: RNA interferece
RT-qPCR: Real time quantitative pcr
SBMA: Spinal and bulbar muscular atrophy
SCA: Spinocerebellar ataxia
SKN-1: Skinhead-1
TFEB: Transcription Factor EB
TORC1: Target of rapamycin complex 1
YA: young adult
YFP: Yellow fluorescent protein

1. Introduction

1.1. Polyglutamine diseases

The generation of proteins is a finely regulated process by which a protein acquires its functional three-dimensional conformation. Any alteration of the sequence, whether by a point mutation or microsatellite expansions (repetitive DNA sequences of 2-9 base pairs), can have consequences on the three-dimensional structure that can trigger the functional loss of the protein. At times, these alterations can cause hydrophobic domains that should be at the core of the protein to become exposed to the aqueous environment, making the molecule prone to aggregating with itself through non-polar interactions, forming fibrils that later evolve into larger aggregates, eventually producing inclusion bodies. As a consequence, they are molecules with a gain of toxic function, as they not only lose their function, but can also force other proteins from the cellular environment to collapse and seriously disrupt protein homeostasis, which is relatively common in several neurodegenerative diseases, like Huntington, Alzheimer and Parkinson (Cox et al., 2020; Ross & Poirier, 2004).

Polyglutamine (polyQ) diseases refer to a set of hereditary neurodegenerative disorders that arise from the unstable expansion of cytosine-adenine-guanine (CAG) trinucleotide repeats, encoding the amino acid Glutamine, in the coding region of the genes causing each polyQ disease. This genetic modification leads to the production of abnormal proteins that have an extended polyQ segment, making them more susceptible to aggregation and capable of causing toxicity. The unstable expansions of polyQs result in neurodegeneration, which causes cognitive and motor impairments. These pathological characteristics differ depending on which area of the brain is affected by the specific disease (Takeuchi & Nagai, 2017). The group includes Huntington disease (HD), dentatorubral pallidoluysian atrophy, spinal and bulbar muscle atrophy and some types of spinocerebellar ataxias (SCAs) (SCA1, SCA2, SCA3, SCA6, SCA7 and SCA17) (Costa & Maciel, 2022).

The range of CAG triplets carried by alleles in healthy and diseased populations varies between different pathologies (Table 1.1). For example, in relation to SCA6, the pathogenic allele may carry between 19 and 33 CAG triplets, a range that is within normal limits for HD, whose minimum pathogenic threshold is reached with 36 CAG triplets or more. In this pathological context, a range from 36 to 38 triplets is considered a diffuse range (incomplete penetrance), while with a number of CAGs equal to or greater than 39 repeats, the penetrance is complete. There is a common correlation in many of these diseases between the length of the CAG repetitive region and the severity or earlier onset of symptoms, with worse prognoses when CAG triplet expansions are longer, as described for SCA2, SCA3, and HD. Therefore, there is an inversely proportional correlation between the length of the CAG repetitive expansion and the age of onset of motor symptoms (P. Giunti, 1998; Maciel et al., 1995; Trottier et al., 1994).

Table 1.1. PolyQ diseases and their causative proteins *(Costa & Maciel, 2022)*

	PolyQ disease	Gene locus	Mutated protein	Pathogenic repeat length
SCAs	SCA1	6p22-23	Ataxin 1	> 39
	SCA2	12q23-24	Ataxin 2	> 31
	SCA3/Machado-Joseph	14q24-31	Ataxin 3	> 55
	SCA6	19p3	CACNA 1 P/ Q-type α 1A	> 19
	SCA7	3p12-21	Ataxin 7	> 37
	SCA17	2q13	TATA box binding protein	> 43
Huntington disease		4p16.3	Huntingtin	> 36-39
DRPLA		12q	Atrophin 1	> 49
SBMA		Xq11-12	Androgen receptor	> 38

All diseases associated with polyQs affect a minority of the population, being considered rare or minority diseases, with the most prevalent being HD (1-10 per 100,000 individuals in Western countries) and the least prevalent being SCA17, with less than 100 affected families estimated worldwide (reviewed on www.orphanet.net, May 2023). The transmission of these pathologies to offspring follows an autosomal dominant inheritance pattern, except in the case of SBMA, which is linked to the X chromosome with dominant inheritance (Fan et al., 2014).

One of the most studied examples has been HD, which is the most prevalent monogenic neurodegenerative disease and the most common genetic form of dementia in developed countries (Ghosh & Tabrizi, 2018). It is caused by the presence of an expansion of 36 or more copies of the CAG triplet in exon 1 of the *HTT* gene that encodes the huntingtin protein (Htt), which confers a toxic gain-of-function to the protein. The mutant Htt (mHtt) is prone to aggregate, becoming a toxic species that accumulates both in the nucleus and cytoplasm of neurons, disrupting the function of effector proteins and cellular processes (G. Vonsattel & DiFiglia, 1998). The regions of the brain most affected by mHtt are the striatum and the cortex (Bohanna et al., 2011).

1.2. *C. elegans* as animal model in biomedical research

Caenorhabditis elegans (*C. elegans*) is a member of the Nematoda phylum, which is the most widespread and diverse group of animals found in almost all habitats (Strange, 2006). It is a tiny free-living soil animal, measuring approximately 1mm in length. The anatomy, genetics and developmental biology of *C. elegans* are well described and it possesses a highly differentiated system (Muschiol et al., 2009). The entire cell lineage of *C. elegans*, from zygote to larva, was already traced in 1983 (Sulston et al., 1983). Hermaphrodite adults have 959 somatic cells, while males have 1031 (Altun et al., 2009), and their nervous system is well known, with 302 neurons in hermaphrodites and 381 in males (J G White et al., 1986).

The genome of *C. Elegans*, the first genome of a completely sequenced multicellular organism (*C. elegans* Sequencing Consortium, 1998), consists of 5 pairs of autosomal chromosomes (I, II, III, IV, V) and the pair of sex chromosomes, which determine whether the organism is hermaphrodite (XX) or male (XO). Males are very rare in nature, as they appear as a result of a failure in the meiotic separation process of the X chromosome, that is, they only have one copy of this chromosome (Baylis & Vázquez-Manrique, 2012).

C. elegans offers several advantages as an animal model in biomedicine, such as its short lifespan. The life cycle lasts only 3 days at 20 °C, but the duration can be modified by varying the cultivation conditions, especially temperature and food availability. These nematodes generate large offspring through sexual reproduction, which can occur by self-fertilization in hermaphrodites or by mating with males.

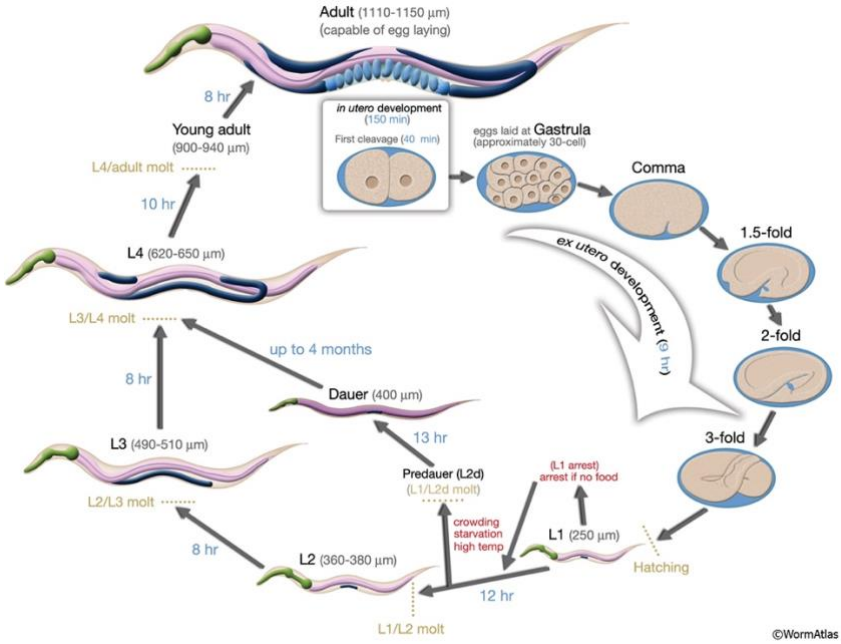

Figure 1.1. Life cycle of hermaphrodite *C. elegans* at 22ºC. The initial stage of development is fertilization at time 0. The duration of each stage is indicated by blue numbers on the arrows. The first cleavage usually occurs approximately 40 minutes after fertilization. The eggs are laid externally during the gastrula stage, which occurs at around 150 minutes after fertilization. The size of the animal during each stage is labeled in micrometers (µm) next to the name of the stage. The time required for the transition from one stage to the next is expressed in hours (hr) and specified in light blue. (Wormatlas.org, May 2022).

The short life cycle of *C. elegans* (figure 1.1) starts when they undergo significant changes from the approximately 30-cell stage when the egg is laid until it hatches and releases the newborn worm. Its postembryonic development is divided into four larval stages (L1, L2, L3, and L4), followed by adulthood. The initial phase of adulthood, called young adult (YA), lasts for around 8 hours, after which the worms become capable of egg laying. In unfavourable conditions such as crowding, high temperature, or starvation, they can transform into dauer larvae for up to four months (Fielenbach & Antebi, 2008). Dauer larvae enter into a resistance stage that allows them to survive the extreme conditions. The dauer larvae recover to become reproductive adults with normal life spans when they are returned to favorable surroundings. The existence of this survival stage is very convenient regarding maintenance and storage of *C. elegans*.

Another advantage is their transparency, which allows for easy visualization of gene expression patterns in living worms by bonding interest genes to reporter molecules such as green fluorescent protein (GFP). Another advantage is their genetic homology with humans, ranging

from 60% to 80% (Avila et al., 2012). *C. elegans* also lends itself to genetic manipulation, such as knockdowns via RNA interference of genes and site-directed mutagenesis using CRISPR (Dickinson & Goldstein, 2016; Fire et al., 1998). Additionally, *C. elegans* can be easily frozen and defrosted alive for long-term storage and can be grown in liquid media for diverse purposes (Brenner, 1974).

C. elegans works as an animal model for polyQ diseases (Morley et al., 2002). The *C. elegans* AM141 strain carries the rmls133 insertion on the X chromosome, which causes the expression of a yellow fluorescent protein (YFP) fused in-frame with 40 glutamines under the muscle promoter *unc-54p*. Since this strain expresses YFP, the aggregates can be observed *in vivo* and in real-time with a microscope with fluorescence. The aggregates accumulate in an age-dependent manner, similarly to the mutant Htt protein in HD patients. These observations can be graphed and used to quantify the phenotype, which can be altered by genetic mutations and drugs.

1.3. AMPK as therapeutic target

AMPK is a heterotrimeric enzyme complex that regulates cellular energy homeostasis and metabolism (Barnes et al., 2002). AMPK is a serine/threonine protein kinase composed of a catalytic subunit, AMPKα, and two regulatory subunits, AMPKβ and AMPKγ. All subunits play a relevant role in regulating AMPK function, which can be activated by a range of different molecules, including AMP, other metabolites, protein kinases, and various drugs (Kim et al., 2016). When cellular ATP levels decrease, circulating AMP levels consequently increase and can specifically bind to the regulatory subunit AMPKγ, inducing enzymatic complex activation to phosphorylate a wide range of targets (Kim et al., 2016).

Once AMPK is activated, it is responsible for controlling metabolism, cell growth, and clearance processes such as autophagy. Precisely, through the autophagic flux, it is able to reduce levels of mHtt (Yamamoto et al., 2006). Likewise, genetic or pharmacological activation of AMPK also induces neuronal protection in an environment of toxicity induced by polyQs in *C. elegans* and reduces cell death in *in vitro* mammalian models of HD, which is associated with a reduction in the number of inclusion bodies (Vázquez-Manrique et al., 2016).

1.3.1. Synergistic activation of AMPK: Metformin and salicylate

Among synthetic activators, metformin is one of the most well-known for indirectly activating the AMPK enzymatic complex (Kim et al., 2016). This substance is a drug universally used to treat type 2 diabetes (Rojas & Gomes, 2013). Metformin induces a moderate inhibition of mitochondrial electron transport chain complex I, increasing AMP levels and therefore activating AMPK (Musi et al., 2002).

However, there are additional ways in which metformin can control metabolism. For instance, in type 2 diabetes patients, metformin alters lipid metabolism by boosting fatty acid uptake in adipose tissue and reducing lipid buildup in skeletal muscle. In patients with non-insulin dependent diabetes, metformin alters a number of metabolic pathways systemically. It may also correct metabolic dysregulation brought on by other diseases, demonstrating a direct link between HD and type 2 diabetes (reviewed by Trujillo-Del Río et al., 2022). Additionally, a cross-sectional study revealed that HD patients receiving metformin treatment for type 2 diabetes have superior cognitive performance than HD patients not receiving metformin treatment (Hervás et al., 2017).

In this sense, several authors have shown that metformin reduces muscular polyQ aggregation and neuronal toxicity in *C. elegans* (Sanchis et al., 2019; Vázquez-Manrique et al., 2016), as well as decreases behavioral defects in mammalian models of Huntington's disease (Arnoux et al., 2018; Sanchis et al., 2019; Vázquez-Manrique et al., 2016).

AMPK activation caused by metformin has been shown to be protective at a concentration of 2000 µM in the context of neuronal and muscular polyQ toxicity in *C. elegans*. (Gómez-Escribano et al., 2020). On the other hand, salicylate, a salt or ester of salicylic acid found in aspirin, can also modulate AMPK activation by allosterically binding to the regulatory subunit AMPKβ (Hawley et al., 2012; Kim et al., 2016). Therefore, metformin and salicylate together can synergistically activate AMPK, as in figure 1.2.

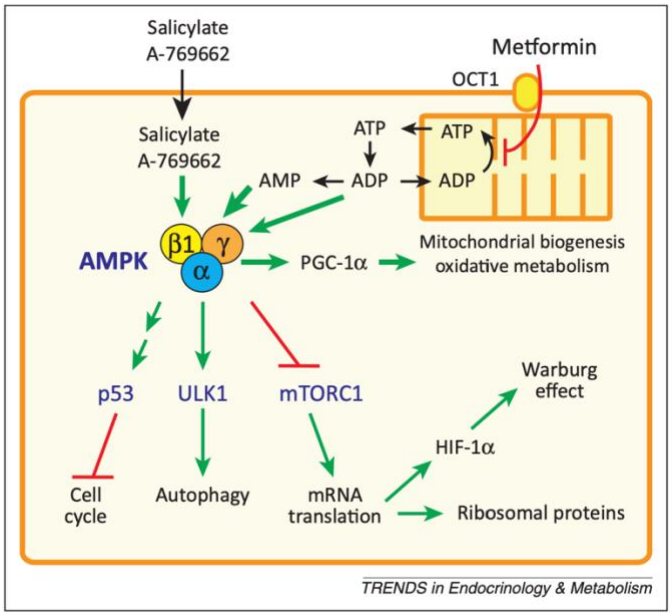

Figure 1.2. Proposed mechanisms by which AMPK activators exert metabolic changes in cells. (Steinberg et al., 2013)

However, metformin and salicylate are pleiotropic substances, so AMPK is not their only target. These drugs have a broad spectrum of action. It is also interesting that they share AMPK as a common target. Furthermore, chronic treatment with these substances is associated with side effects (Bray et al., 2012; Huang et al., 2011). Therefore, the possibility of reducing the dose of both compounds, even when administered in combination, could greatly reduce unwanted effects.

Gómez-Escribano et al. (2020) achieved a pharmacological synergistic activation of AMPK with a dose decrease of roughly 10 times for each agent. The dosage of the medicines used is decreased in order to avoid activating unwanted targets while still reducing polyQ-induced toxicity, lengthening the life span and regaining neural function in *C. elegans*.

Moreover, they found that AMPK catalytic subunit (aak-2/AMPKα2, in *C. elegans* and human respectively) is required for the protection exerted by both drugs (Gómez-Escribano et al., 2020), as loss of function mutants of aak-2/AMPKα2 do not respond to the treatment. Confirming the interaction of metformin and salicylate with AMPK. This work also showed that autophagy flux is needed for the synergistic effect of both drugs in polyQ aggregation and mobility. However further study needs to be done to clarify if AMPK activation promotes autophagy to reduce the aggregation and increase mobility or whether both processes run at the same time.

The experiments described by Gómez-Escribano et al (2020) were carried out in liquid media. The administration via is relevant in the effect caused by the metformin and salicylate treatment. Treating worms in solid media can produce changes in the pharmacological efficacy and in the response to metformin and salicylate. Moreover, worms are under additional stress in liquid media, therefore, it is important to validate those results in solid media.

1.4. Autophagy as protein clearance mechanism

Homeostasis in cells, tissues, and organisms is fundamentally influenced by the lysosomal breakdown pathway of autophagy, which is controlled by genes associated to autophagy (ATG) that have been preserved throughout evolution. Mutations in the genes that regulate autophagy have been definitively linked to human disease (Levine & Kroemer, 2019). Problems in the autophagic flux may result in disease since autophagy targets harmful proteins, intracellular bacteria, and malfunctioning organelles specifically.

It is the main intracellular catabolic mechanism for degrading and recycling defective proteins, such as misfolded mHtt. During autophagy, faulty molecules and organelles are marked for degradation. They are then enclosed in phagosomes, which mature into autophagosomes and fuse with lysosomes, exposing them to the lysosomal content for degradation. Dysregulation of autophagy can lead to inflammation, aging, metabolic disorders, neurodegenerative disorders, and cancer (Condello et al., 2019). The presence of mHtt aggregates causes cellular stress by disrupting protein homeostasis, and regulatory mechanisms should act to restore this imbalance. However, an impairment of autophagic flux has been described due to the presence of mHtt, preventing the elimination of the aggregates (Martinez-Vicente et al., 2010).

There are multiple genes regulated by AMPK downstream effectors that take part in autophagy, so their expression can be used as a measure of the activation of autophagic process (Zhang et al., 2015). These genes include the ATG genes, such as *atg-9*, *atg-18, lgg1-1* and *sqst-1* in *C. elegans*. The process of development of sealed autophagosomes that will merge with lysosomes is dependent of ATG genes, and their roles in various membrane trafficking and signalling pathways also have significant consequences for cell biology, physiology, and disease (Levine & Kroemer, 2019).

The *lgg-1* gene actively participates in the formation of autophagosomes and is essential during the activation of the autophagic process in *C. elegans.* This gene belongs to a family of homologs that includes the ATG8 gene in Saccharomyces cerevisiae and the LC3 protein in mammals (Tanida et al., 2008). SQST1 (an ortholog of the mammal p62) has an important role in proteotoxic stress response and aging, and it is capable of inducing autophagy (Kumsta et al., 2019).

1.5. AMPK downstream effectors

There are different AMPK downstream effectors implicated in the processes of autophagy and oxidative stress response. AMPK is a master regulator of healthspan and lifespan modulating energy metabolism, stress resistance and cellular proteostasis. AMPK activates signalling of *Nrf2*/SKN-1, *FoxO*/DAF-16 and indirectly activates the autophagy regulator HLH-30 by inhibiting the *mTOR*/LET-363 pathway (Salminen & Kaarniranta, 2012). The pathways can be seen in figure 1.3.

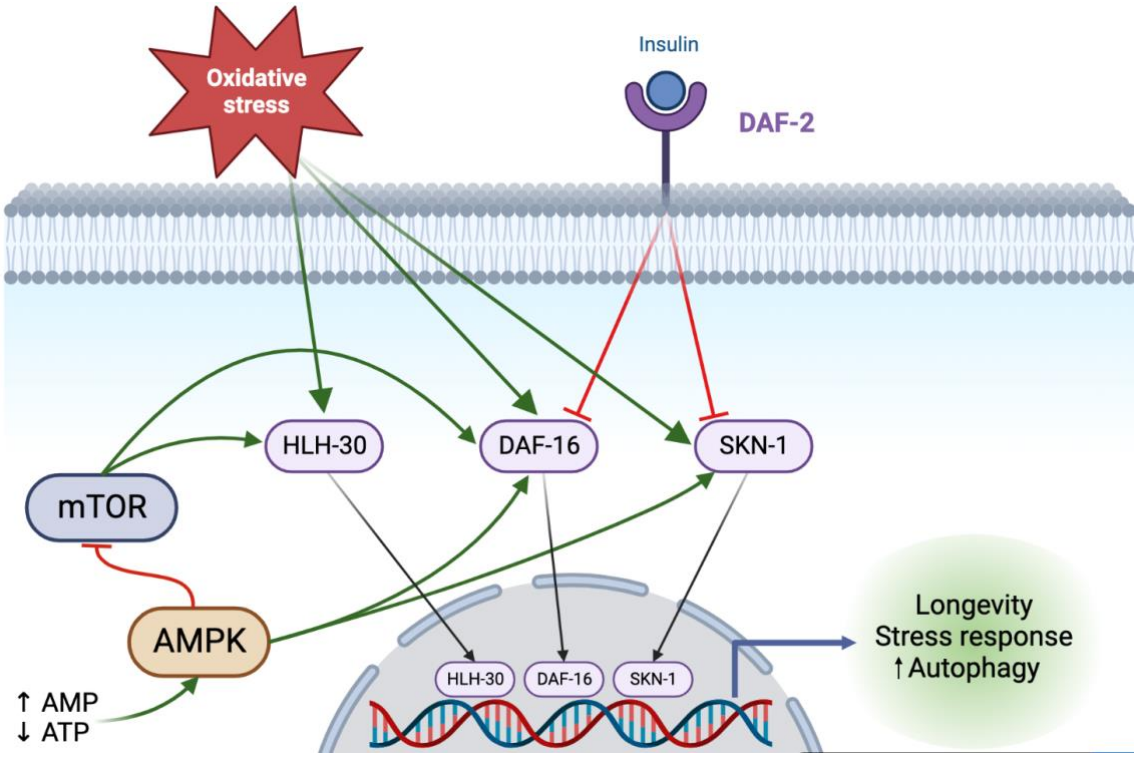

Figure 1.3. Graphic representation of AMPK downstream effectors. Generated in BioRender.com. (Adapted from Franco-Juárez et al., 2021; Hesp et al., 2015; Hwang et al., 2022; Salminen & Kaarniranta, 2012)

DAF-16, the sole homolog of the forkhead box transcription factor class O (*FoxO*) in *C. elegans*, integrates signals from upstream pathways to induce transcriptional alterations in several genes involved in metabolism, immunity, stress, aging, and development (Zečić & Braeckman, 2020). The major regulator of DAF-16 activity is the insulin/insulin-like growth factor 1 (IGF-1) signaling (IIS) pathway. When this pathway is reduced, it promotes lifespan extension in worms, flies, mice, and humans.

DAF-16 combines signals from numerous upstream pathways that function concurrently with IIS. AMPK can directly phosphorylate DAF-16 to activate it. It has been demonstrated that DAF-16 is phosphorylated by AMPK *in vitro* at at least six distinct residues (Greer et al., 2007a). DAF-16 is also a target of the TOR signaling pathway. Genetic suppression of TORC1 extends lifespan by increasing daf-16 transcription and causing nuclear translocation. This longevity trait also needs SKN-1 to be activated in addition to DAF-16 (Robida-Stubbs et al., 2012). Moreover, it was demonstrated that activation and nuclear translocation of DAF-16 were necessary for the lifespan extension (Ogg et al., 1997). The genes targeted by AMPK-DAF-16 pathway are mainly associated with increased lifespan. This includes genes involved in resistance against oxidative stress (Li et al., 2009), as well as against DNA damage, such as Gadd45a (Tran et al., 2002).

SKN-1 has a high degree of homology with the human nuclear factor erythroid 2-related factor (Nrf2). This multifunctional regulator is thought to be a cytoprotective factor that controls the expression of genes encoding antioxidant, anti-inflammatory, and detoxifying proteins, and is as well, a potent modulator of species longevity. When promoting lifespan extension, SKN-1 functions in two ASI neurons under dietary restriction conditions. SKN-1 also exerts an effect in the intestine to increase longevity in oxidative stress conditions and in a context of reduced insulin pathway signalling (Bishop & Guarente, 2007).

Onken & Driscoll (2010) report that metformin activates AMPK to induce SKN-1 nuclear translocation and expression of *gst-4* (a target of SKN-1) in intestine. They suggest that metformin needs SKN-1 activities in both ASI neurons and intestine in order to extend healthspan.

Given normal circumstances SKN-1 is confined to the cytoplasm, but in reaction to stressful situations, such as when exposed to H_2O_2, it translocates to the nucleus. Through a basic region, it attaches to DNA in the nucleus (to the consensus WWTRTCAT (W being A or T, R being G or A) sequence) as a monomer (An & Blackwell, 2003).

The basic helix-loop-helix transcription factor HLH-30 is a conserved ortholog of the mammalian transcription factor EB (TFEB). It is a key regulator in lipid metabolism during starvation conditions, regulates the expression of genes involved in the autophagy process and increases lifespan in several longevity pathways (Lapierre et al., 2013). It also mediates resistance to several stress elements besides starvation, such as oxidative and heat stress, and host defence against pathogen infection (Lin et al., 2018).

HLH-30/TFEB is a direct target of mTOR phosphorylation forcing it to remain in the cytoplasm, but as a consequence of reduced mTOR signalling, the repressive phosphorylation is removed and HLH30 translocates to the nucleus (Lapierre et al., 2013; Martina et al., 2012). Since there is strong evidence that AMPK inhibits mTOR (Cork et al., 2018), HLH-30 can be indirectly translocated by AMPK activation.

The identification of these mentioned AMPK effectors as key transcription factors that regulate different genes involved in the autophagy process supports the concept that higher autophagic flux and AMPK activation are possibly essential to ensure extended lifespan.

2. Objectives

The global objective of this project is to evaluate the efficiency of synergistic treatment of metformin and salicylate in solid media and to deepen into the AMPK downstream effectors involved in the development of the pharmacological response, since both drugs act pleiotropically and it is unclear whether alternative signaling pathways may be involved.

To this end, the following specific aims were defined:

1. Evaluation of synergistic treatment with metformin and salicylate in solid media.
2. Quantification of autophagic flux through fluorescence microscopy.
3. Determine the implication of DAF-16 in the response through fluorescent markers and RNA interference.
4. Study of the subcellular localization of AMPK targets, HLH-30 and SKN-1, through the use of fluorescent markers.
5. Study the expression of autophagy-related genes after treatment with metformin and salicylate.

3. Materials and methods

3.1. *C. elegans* maintenance

The manipulation and maintenance of the strains included in this work have been carried out according to the described specifications (Brenner, 1974). The Nematode Growth Medium (NGM) has been used for the growth and maintenance of the nematodes. Its composition listed in table 3.1. and the medium was sterilized before adding $CaCl_2$, $MgSO_4$, KPO_4, cholesterol and nystatin. Table 3.2 contains a detailed description of each of the strains used. Practically all the strains generated in Dr. Rafael Vázquez's laboratory (denoted as "RVM") have been crossed in successive rounds (>3) with the reference wild genome, Bristol N2, to avoid carrying any unintended mutations. The animals have been maintained at 20 °C for all experiments, unless stated otherwise.

Table 3.1. NGM media components

Component	Concentration	Source
Bacteriological agar	20 g/L	Condalab (Madrid, Spain)
NaCl	3 g/L	Condalab (Madrid, Spain)
Peptone	2.5 g/L	Condalab (Madrid, Spain)
$CaCl_2$	1 mM	Sigma Aldrich (St. Louis, MI, EE. UU.)
MgSO4	1 mM	Sigma Aldrich (St. Louis, MI, EE. UU.)
KPO_4	15 mM	Sigma Aldrich (St. Louis, MI, EE. UU.)
Cholesterol	5 mg/ml	Sigma Aldrich (St. Louis, MI, EE. UU.)
Nystatin	12.5 mg/ml	AppliChem GmbH (Ottoweg, Germany)

Table 3.2. Worm strains used in this study.

Name	Genotype	Description	Reference
Bristol N2	Wild type	Reference wild strain	(Brenner, 1974)
AM141	*rmIs133 [unc-54p::40Q::YFP]-X*	It expresses 40Q bound to YFP under the muscular promoter unc-54p	Morley 2002
RVM455	*rmIs133 [unc-54p::40Q::YFP; aak-2 (ok524)-X*	It expresses 40Q bound to YFP under the muscular promoter unc-54p and contains a deletion for AMPK α subunit	Pending to be published
DA2123	*adIs2122 [lgg-1p::GFP::lgg-1+rol-6 (su1006)]*	It expresses GFP bound to LGG-1 and they are rollers so can be selected	Caenorhabditis Genetics Center (CGC, Minneapolis, MN, USA)
RVM537	*adIs2122 [lgg-1p::GFP::lgg-1 + rol-6(su1006)];aak-2 (ok524)*	It expresses GFP bound to LGG-1, they are rollers so can be selected and contains a deletion for AMPK α subunit	Pending to be published

VZ892	*syb1452 [hlh-30::3xFLAG::eGFP]) IV*	It expresses GFP bound to HLH-30	Caenorhabditis Genetics Center (CGC, Minneapolis, MN, USA)
TJ356	*zIs356 [daf-16p::daf-16a/b ::GFP+rol-6 (su1006)]*	It expresses GFP bound to DAF-16 and they are rollers so can be selected	Caenorhabditis Genetics Center (CGC, Minneapolis, MN, USA)
LD1	*ldIs7 [skn-1b/c::GFP+rol-6 (su1006)]*	It expresses GFP bound to SKN-1 and they are rollers so can be selected	Caenorhabditis Genetics Center (CGC, Minneapolis, MN, USA)

3.1.1. Worm culture

The food for *C. elegans* was prepared from a liquid culture of the OP50-1 bacteria, which is resistant to streptomycin. For this purpose, a colony was selected from a triple streak and inoculated into a flask containing LB liquid medium, the composition of which is specified in table 3.3. This culture was incubated overnight at a temperature of 37 °C and under agitation conditions at 180 rpm. The next day, 1 mL was seeded onto each 60 mm NGM plate and 300 µl onto 35 mm plates.

Table 3.3. Liquid LB composition.

Component	Concentration	Source
Tryptone	10 g/L	Condalab (Madrid, Spain)
NaCl	10 g/L	NZYTech (Lisboa, Portugal)
Yeast extract	5 g/L	Condalab (Madrid, Spain)

To ensure an adequate amount of food, the worms were regularly transferred to clean NGM plates seeded with OP50-1 bacteria. For this, a portion of agar from an NGM plate was cut and transferred to a new NGM plate with food.

3.1.2. Population synchronization

To obtain synchronized worm populations, hermaphrodites carrying eggs inside them were collected by washing the Petri dishes where the animals were cultured using 1X M9 solution (detailed in table 3.4). Subsequently, the worms were transferred to 15 mL conical tubes. The tubes were centrifuged at 1500 rpm for 1 minute to recover the animal pellet. The supernatant was removed using a 10 mL serological pipette, and a volume of 4 mL of a diluted synchronization solution (table 3.5) containing 12.5% sodium hypochlorite (NaClO) was added to the pellet. The animals were lysed at room temperature for a maximum of 5 minutes to avoid undesired toxic effects from the bleach. To promote complete cuticle rupture, the tubes were vigorously and manually shaken, ensuring friction of the medium against the tube wall. Subsequently, the lysed sample was centrifuged at 1500 rpm for 1 minute to remove residual bleach. Afterwards, the sedimented eggs were washed at least twice with 1X M9 to dilute the bleach concentration in the samples. In the final step, the egg pellet was suspended in 2 mL of residual 1X M9 from the washes and incubated at 20°C with automatic agitation overnight to promote hatching of the eggs, which will give rise to synchronized L1 populations.

Table 3.4. M9 buffer composition

Component	Concentration	Source
Na_2HPO_4	6 g/L	Scharlau (València, Spain)
KH_2PO_4	3 g/L	Sigma Aldrich (St. Louis, MI, EE. UU.)
NaCl	5 g/L	NZYTech (Lisboa, Portugal)
$MgSO_4$	1 mM	Sigma Aldrich (St. Louis, MI, EE. UU.)

Table 3.5. Bleach solution

Component	Amount	Source
NaClO	1 mL	Sigma Aldrich (St. Louis, MI, EE. UU.)
NaOH 1M	2.5 mL	Thermo Fisher Scientific, Waltham, MA, USA)
H_2O	0.5 mL	-
M9 1X	4 mL	Prepared at lab

For the stains that were too weak to tolerate the toxic effect of the bleach, alive gravid hermaphrodites (carrying eggs) were transferred using a platinum wire to new plates for 2 hours. After they had laid eggs, the animals were removed, obtaining a synchronized worm population.

3.2. Pharmacological assays with metformin and salicylate

To study the effect of synergistic activation of AMPK, 35 mm plates were prepared with NGM with 0.005 mM salicylate and 0.15 mM metformin (both from Sigma-Aldrich ((St. Louis, MI, EE. UU.)). For the positive control, plates with 2 mM metformin were prepared, and with water for the negative control. Afterwards, OP50-1 bacteria were seeded as described before and around 100 animals were added. Worms were maintained at 20 ºC until they reached young adult stage.

3.3. RNA interference of daf-16

The animals were fed with the *E. coli* HT115 strain that contains an IPTG-inducible T7 RNA polymerase and is deficient in the RNase III enzyme (Timmons et al., 2001). The HT115 strain was transformed with the pL4440 plasmid, which contains two promoter sequences for the T7 RNA polymerase flanking the insertion site (Figure 3.1.). Once induced by IPTG, the RNA polymerase synthesizes a specific double-stranded RNA corresponding to the gene intended for interference.

3.3.1. Genomic DNA Extraction and Amplification

Genomic DNA was required to use as a template in PCR to amplify the gene regions desired to be cloned into expression vectors. Genomic DNA was extracted from wild-type strains (N2) using the commercial kit DNeasy Blood & Tissue from QIAGEN (Hilden, Germany). The amplicon (267 bp) was amplified using a high-fidelity Taq DNA polymerase (Phusion® High Fidelity, Thermofisher Scientific) and specific primers (table 3.5) designed targeting exons common to all isoforms to promote the silencing of all of them. The PCR product was purified using the kit *QIAquick PCR Purification Kit* from *Qiagen* (Hilden, Germany), and quantification was performed using the NanoDrop2000 spectrophotometer (Thermo Fisher Scientific, Waltham, MA, USA).

Table 3.5. Primers used for RNA interference of gene *daf16*.

Gene	Primer	Type	Sequence	Tm
daf-16	CTR1279	forward	5' CGA TTG CCG GAT CGA TTC AAA CG 3'	58 ºC
	CTR1280	reverse	5' CAT GGG TTG GCG AAT CGG TTC C 3'	

3.3.2. Vectors

The pL4440 vector was used in this project to obtain the necessary RNAi construct. The vector contains ampicillin resistance gene, allowing for the selection of bacteria that have incorporated the plasmid.

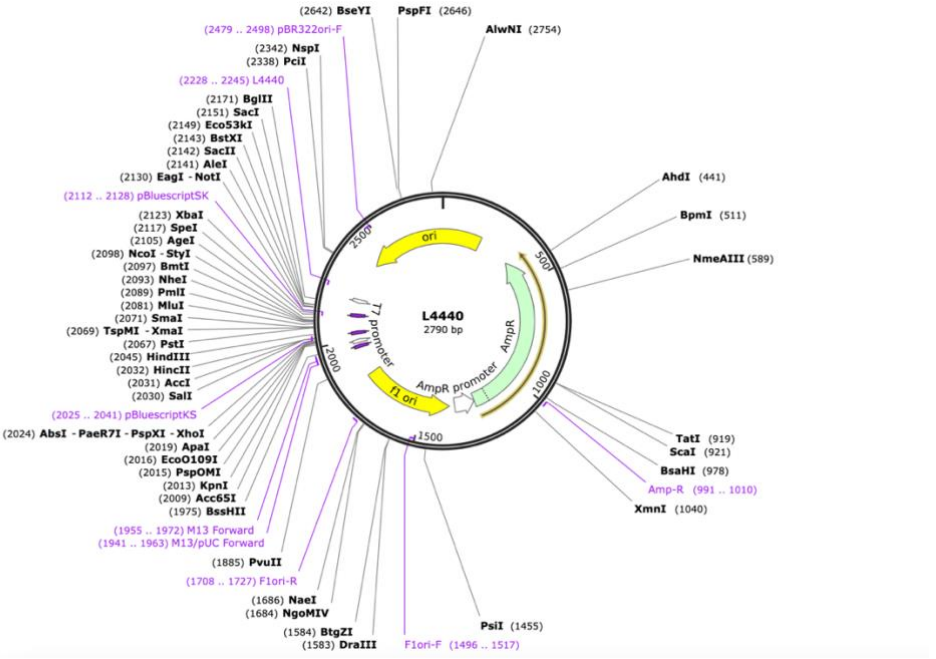

Figure 3.1. Diagram of plasmid L4440 used for RNA interference in C. elegans. The vector was deposited in Addgene by Andrew Fire lab (Addgene, 2023)

3.3.3. Vector Digestion and Insert Ligation

The amplicon was cloned into the pL4440 vector using the EcoRV restriction enzyme which generates blunt ends upon cleavage. Ligation was performed using the T4 DNA ligase enzyme. The appropriate vector concentration was 100 ng, and the vector-insert ratio was 3:1. The reaction mixture, detailed in Table 3.6., was incubated overnight at room temperature. After enzyme inactivation at 65 °C for 10 minutes, bacterial transformation was performed.

Table 3.6. Reaction mix for restriction-ligation procedure

Reagent	Concentration	Source
pL4440	100 ng	-
Insert	28.7 ng	-
T4 DNA ligase buffer	0.05 UI/µl	NZYTech (Lisboa, Portugal)
T4 DNA ligase enzyme	1X	NZYTech (Lisboa, Portugal)
EcoRV enzyme	0.05 UI/µl	Thermo Fisher Scientific (Waltham, MA, EE. UU.)
H2O	Up to 20 µl	-

3.3.4. Transformation

Electrocompetent bacteria were prepared from the *E. coli* HT115 strain, which was necessary to introduce the desired construct into them. The competent bacteria were aliquoted in 50 µL per tube and stored at -80°C.

To carry out the electrotransformation process, 0.6 µL of the ligation reaction was added to the thawed competent bacteria, and then the volume was introduced through the slot of the pre-cooled electroporation cuvette. The cuvette was placed in the electroporator, and the voltage was set to 1800 V. Next, the transformed bacteria were recovered with 900 µL of LB and incubated for 45 minutes at 37 °C. Finally, 80 µL were plated on selective medium containing ampicillin, resistance provided by the vector. The remaining bacteria were centrifuged at 7000 rpm for 1 minute and then, half of the supernatant was removed. The cells were resuspended and plated on the same selective media for higher concentration. Plates were incubated overnight at 37 °C.

3.3.5. PCR analysis of colonies obtained from transformation.

This type of PCR was used for rapid screening of the fragments inserted into pL4440, directly from colonies derived from *E. coli* HT115. The first step of the reaction, denaturation, needed to be prolonged to allow for the lysis of the bacterial wall and release of the plasmid, which served as a template in the PCR. Using a sterile pipette tip, an isolated colony was touched, deposited in a new plate divided into squares so it is possible to recover the positive colonies after PCR, and finally, the tip was introduced into the PCR cocktail by agitation. The components of the PCR are described in table 3.7 and PCR program is detailed in table 3.8. The primers used were M13 forward (5´-GTAAAACGACGGCCAG-3´) and CTR1280 (table 3.5) as reverse.

Table 3.7. Components of PCR for colony selection

Reagent	Concentration	Source
H_2O	Up to 24 µl	-
Buffer	1X	Biotools (Madrid, Spain)
$MgCl_2$	1.5 mM	Biotools (Madrid, Spain)
dNTPs	0.2 mM	NZYTech (Lisboa, Portugal)
Direct primer M13	0.4 µM	IDTDNA (Coralville, IO, USA)
Reverse primer 1280	0.4 µM	IDTDNA (Coralville, IO, USA)
Taq polymerase	1.25 U/25 µl	Biotools (Madrid, Spain)

Table 3.8. PCR program for colony selection

Stage	Temperature (Cº)	Time (minutes)	Cycles
Initial denaturation	95	5	1
Denaturation	95	0.5	35
Annealing	58	0.5	
Elongation	72	0.75	
Final elongation	72	5	1
Resting	10	∞	1

Electrophoresis of the product obtained by the PCR is performed in 1% agarose gels in TBE 1X (Invitrogen (MA, USA)). The nucleic acid dye SYBR Safe (Thermo Fisher Scientific (Waltham, MA, USA)) is added to the gel mixture to enable band visualization. Loading buffer (NZYtech (Lisbon, Portugal) is added to each probe and 10 µL of this mix is loaded in each well. To know the fragments size, a molecular marker, GeneRuler 1Kb Plus AND Ladder (Thermo Fisher Scientific

(Waltham, MA, USA)), is also loaded in the gel. Electrophoresis is performed under the following conditions: 120 V, 100 mA and 25 minutes. For band visualization a UV light transilluminator (Bio-Rad Laboratories (Hercules, CA, USA)) is used.

Two of positive colonies were recovered. Using a sterile pipette tip, each of the positive colony from the second plate was touched and inoculated into 6 mL of LB with ampicillin. The culture was kept at 37 °C with agitation (220 rpm) overnight.
To purify plasmid vectors, a miniprep was performed using the bacterial culture. The extraction and purification were carried out using the QIAprep Spin Miniprep Kit from Qiagen (Hilden, Germany). Then, nucleic acids were quantified with NanoDrop2000 spectrophotometer (Thermo Fisher Scientific, Waltham, MA, USA).
Finally, the selected positive clones were validated by Sanger sequencing (STAB vida company, Lisbon, Portugal). From the two sequenced clones, one was selected to continue with the RNAi assay.

3.3.6. RNA Interference Protocol

The Petri dishes in which the nematodes grew in these assays were designed differently from those specified in section 3.2. In this case, 1 mM IPTG (#I5502; Sigma-Aldrich-Merck) was added to induce the activation of the RNA polymerase that produces the double-stranded RNA. Additionally, the necessary drugs for the synergy were added to achieve a final concentration of 0.15 mM metformin and 5 µM salicylate, or their respective control, H_2O for negative and 2 mM metformin for positive.

To obtain bacterial cultures used as worms' food, the generated vector, and the empty vector (negative control) included in HT115 were grown in LB supplemented with 50 µg/µL ampicillin overnight at 37 °C. Subsequently, the grown bacterial cultures were induced with IPTG for 2 hours at 37 °C to promote the synthesis of double-stranded RNA. The compound IPTG is photosensitive, so it is recommended to work under dark conditions whenever possible. The induced cultures were centrifuged at 4000 rpm for 10 minutes to concentrate the bacterial extract. Finally, the bacterial pellet was dissolved in 3 mL of residual LB medium, of which 300 µL were seeded per plate. After approximately 30 minutes of drying in a laminar flow hood, synchronized animals were added to the RNAi plates and cultured at 20 °C in darkness until reaching the young adult stage. To properly interpret the results, it is important to consider that the diet with HT115 per se modifies the basal pattern of polyQ aggregation (Muñoz-Lobato et al., 2014).

3.4. Genetic expression analysis

3.4.1. RNA extraction

The gene expression of two strains was evaluated, AM141 and 455, both cultured with H_2O and metformin and salicylate. To evaluate endogenous gene expression, the population was synchronized, and the animals were collected for washing using 1X M9 buffer. All samples were frozen in lysis buffer (RNA extraction kit; #R6834-01, OMEGA Bio-Tek, Norcross, GA, USA) supplemented with 1% β-mercaptoethanol to induce nematode cuticle rupture. Subsequently, the samples were lysed using 2 cycles of sonication of 15 seconds. RNA extraction was performed using the RNeasy Mini Kit (Qiagen, Hilden, Germany) following the manufacturer's instructions. After completing this process, quantification and estimation of RNA quality were performed using Nanodrop 2000 spectrophotometer (Thermo Fisher Scientific, Waltham, MA, USA).

3.4.2. Reverse Transcription

RNA samples were diluted in RNase-free water to obtain 1 ng of RNA in a total volume of 5 µl. Subsequently, cDNA was obtained from the RNA samples by reverse transcription with a PrimeScript™ RT reagent kit (Takara Bio (Kusatsu, Japan)). The reaction was carried out using 2 µl buffer, 2 µl random 6-mers, 0.5 µl oligo dT and 0.5 µl Reverse Transcriptase. The temperature protocol was 15 minutes at 37 ºC, 5 seconds at 85 ºC and 30 minutes at 10 ºC. Then, samples were stored at -20 ºC.

3.4.3. Real-Time Quantitative PCR

To assess the differential expression of multiple genes, real-time quantitative PCR (qPCR) was employed, enabling relative quantification of the target sequence during amplification.
Four target genes related to autophagy (*atg-9, atg-18, sqst-1* and *lgg*-1) were amplified and the endogenous control *pmp-3* was employed to normalize gene expression levels. The qPCR analysis of gene expression is based on relative quantification, comparing the expression of the target gene in the samples to the expression of the endogenous control (*pmp-3*), which exhibits more stable expression in the analysed samples. Therefore, four TaqMan probes were designed for this procedure.
The qPCR reactions were performed in 96-well plates, with each well containing 15 µL of the reaction mixture. Including 0.75 µl TaqMan probe, 5.75 µl RNase-free water, 7.5 µl 2X PrimeTime® Gene Expression master mix (#RR390, Takara Bio) and 1 µl cDNA. The real-time PCR reaction was performed using the ViiA7 thermocycler (Applied Biosystems, Waltham, MA, USA). The standard PCR program was applied: 1 cycle of 10 minutes at 50 ºC, 1 cycle of 15 seconds at 95 ºC and 40 cycles of 1 minute at 60 ºC.

3.5. Microscopy techniques

Different microscopy techniques were employed in this study. The Leica S6E binocular microscope (Leica, Wetzlar, Germany) was regularly used for the maintenance, manipulation, and observation of C. elegans.
The transgene *unc-54p::40Q::YFP* in AM141 induces inclusion bodies formation in muscle cells in an age-dependent way. Inclusion bodies can be visualized and counted in animals from L2 to adult at real time thanks to the expression of YFP. In this project aggregates (circular bright spots) have been scored in young adult worms using a fluorescence magnifying glass Leica M165 FC (Leica (Wetzlar, Germany)).
The Leica DM6 B (Leica (Wetzlar, Germany)) was used to observe and take images of translocation of the different studied proteins in the strains that had these proteins bound to GFP.

3.6. Image analysis

The images obtained from the hypodermal seam cells of LGG-1::GFP were processed to obtain the number of punctate per cell with the Fiji/Image J software (Schindelin et al., 2012).

3.7. Statistical analysis

The statistical software GraphPad (GraphPad Software, La Jolla, CA, USA) was used to analyse the obtained data and visualize them in graphs. To examine numerical data, an analysis of variance (ANOVA) was used, with Turkey correction for multiple comparisons. One-way ANOVA allows to

contrast the null hypothesis (no difference between populations) with the alternative hypothesis (the populations averages are different) in more than two populations. In this way, it is possible to prove which strain are responsive to treatment. For a *p*-value lower than 0.05 and F test value different from 1, the null hypothesis was refused to confirm the alternative hypothesis.

4. Results

4.1. Reduction of polyQ aggregation in worms treated with metformin and salicylate is maintained in solid media.

AM141 (rmIs133[*unc-54p::40Q::YFP*]-X) worms, which contain an insert of 40 polyglutamines linked to YFP under a muscular promoter (shown in figure 4.1), were cultured since early stages (L1) in solid media containing 2 mM metformin and in a synergic mixture composed of 0.15 mM metformin and 0.005 mM salicylate (from now on the mixture will be designated as synergy). Media containing water was used as control, because water is the administration vehicle in which metformin and salicylate are dissolved. The number of aggregates per worm was visually counted using a fluorescence microscope. The results showed a significant reduction of the number of polyQ aggregates in treated worms in contrast to untreated (figure 4.2).

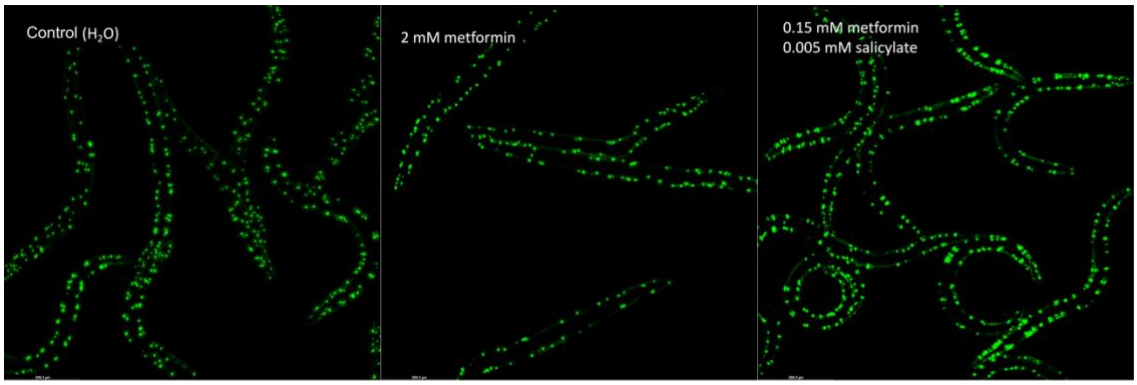

Figure 4.1. Representative images of 40Q::YFP (rmIs133[*unc-54p::40Q::YFP*]-X)) young adult worms in solid media. They were treated with 2 mM metformin and synergy, in which a different polyQ aggregation pattern can be appreciated in body wall muscles. Water works as control. Images were taken using a Leica DM6 B fluorescence microscope at 10x and with an exposure of 100 ms. The brightness and contrast values were modified with Fiji software to improve visualization.

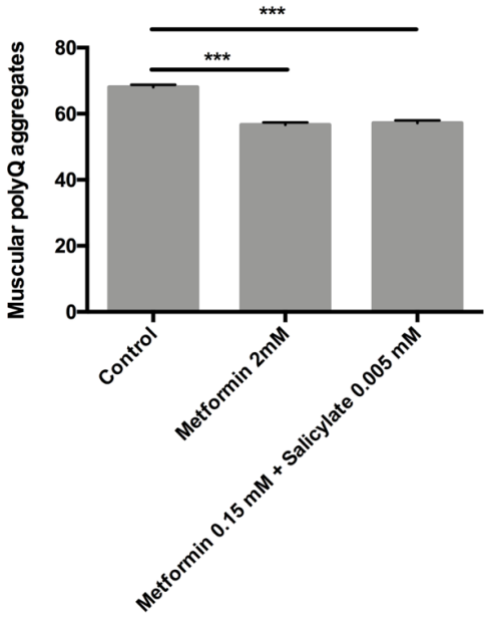

Figure 4.2. Variation in the average number of muscular polyQ aggregates in *rmIs133[unc-54p::40Q::YFP]-X* worms cultured in solid media. Treatment with synergy in solid media can reduce polyQ aggregation compared to untreated worms and provides the same level of protection than 2 mM metformin. The statistical analysis was carried out using ANOVA with Turkey correction for multiple comparisons. At least 50 animals were tested and 6 different experiments were performed in each case. Error bars show the standard error of the mean. ***: *p*-value < 0.001.

4.2. AMPK activity is necessary for the beneficial synergistic effect of metformin and salicylate on polyQ aggregation.

The strain expressing 40Q (*rmIs133[unc- 54p::40Q::YFP]-X)* and the strain 40Q with defective aak-2/AMPKα (*rmIs133[unc- 54p::40Q::YFP ; aak-2(ok524) X*) were cultured and the number of aggregates were visually counted in untreated and treated worms with synergy, as seen in figure 4.3.

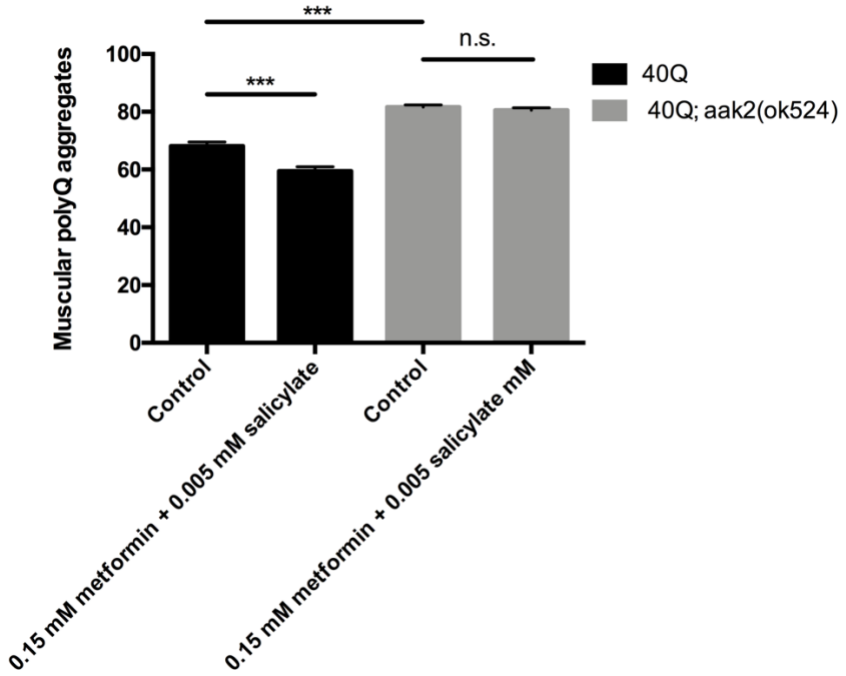

Figure 4.3: Variation in the average number of muscular polyQ aggregates in 40Q and 40Q; *aak2(ok524)* worms. Water was used as control. Treatment with synergy in solid media reduces polyQ aggregation compared to untreated worms in the 40Q strain. However, the rescue does not happen in the *aak-2* mutant. The statistical analysis was carried out using ANOVA with Turkey correction for multiple comparisons, from 5 independent experiments of at least 10 worms for each condition. Error bars show the standard error of the mean. ***: *p*-value < 0.001; n.s.: non-significant (*p*-value ≥ 0.05).

This suggests AMPK is essential in the response triggered by metformin and salicylate to reduce polyQ toxicity.

4.3. Synergistic treatment with metformin and salicylate induces activation of autophagy

As AMPK is known to positively regulate autophagy, it is interesting to check if this process is the responsible mechanism of aggregate clearance when AMPK is synergically activated. To obtain accurate insights of AMPK-activated autophagy upon treatment, autophagy was measured by different means. Autophagy can be indirectly measured by observing GFP-positive punctate areas in LGG1::GFP worms that indicate autophagosomal structures in hypodermal seam cells (Klionsky et al., 2008), as in figure 4.4.B. The number of LGG-1 punctate per seam cell was counted and normalized to the average value of control (water). Incubation at 37 ºC for 1 hour was used as positive control since heat shock induces autophagy. The results can be observed in figure 4.5.

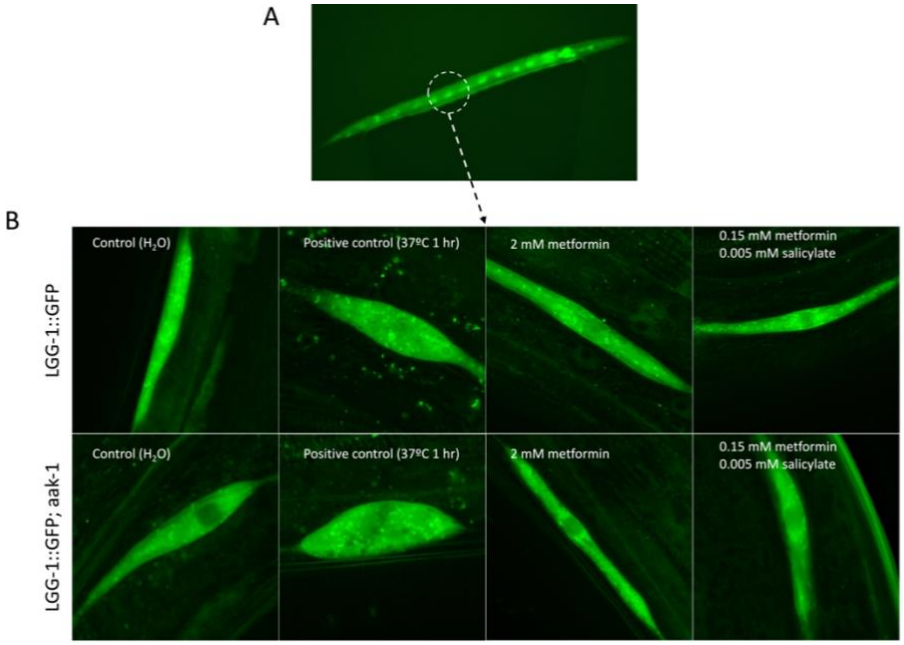

Figure 4.4. Representative images of LGG1::GFP and LGG1::GFP; *aak-2.* A. Representative image of LGG1::GFP (*adIs2122 [lgg-1p::GFP::lgg-1 + rol-6(su1006)]*) at 20x**. B.** Representative zoomed images of seam cells of LGG1::GFP (*adIs2122 [lgg-1p::GFP::lgg-1 + rol-6(su1006)]*) and LGG1::GFP; *aak-2(ok524) (adIs2122 [lgg-1p::GFP::lgg-1 + rol-6(su1006)]; aak-2(ok524))* young adult worms treated with 2mM metformin or synergy. 1 hour at 37ºC is used as positive control. Images were taken using a Leica DM6 B fluorescence microscope at 63x and with an exposure of 100 ms. After image analysis, brightness and contrast values were modified with Fiji software for better punctate visualization.

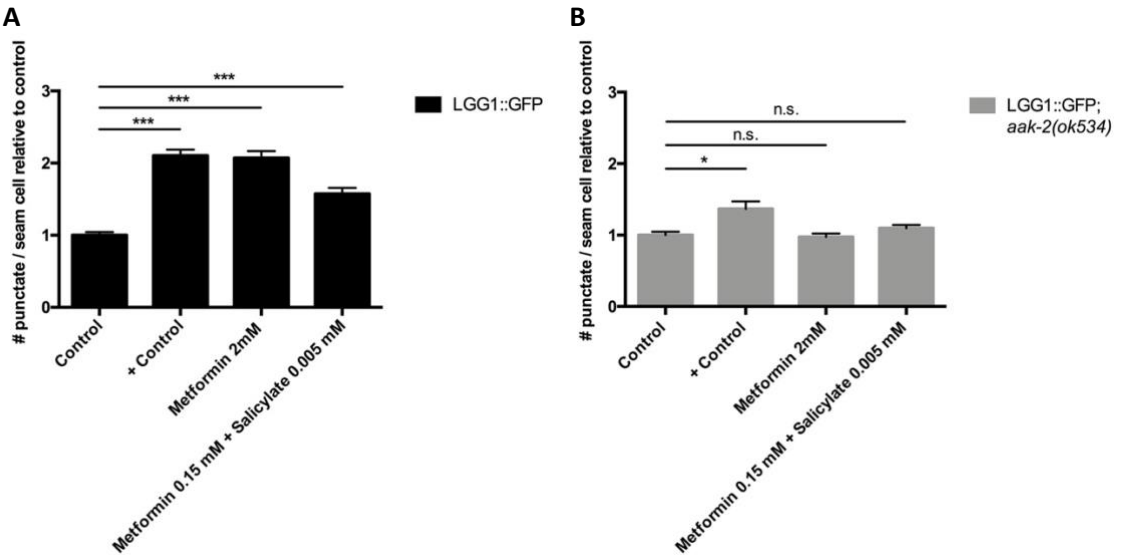

Figure 4.5. Analysis of the average number of punctate per seam cell. A. Analysis of the average number of punctate per seam cell relativized to control in LGG1::GFP (*adIs2122 [lgg-1p::GFP::lgg-1 + rol-6(su1006)]*) young adult worms. **B.** Analysis of the average number of punctate per seam cell relativized to control in LGG1::GFP; *aak-2(ok524) (adIs2122 [lgg-1p::GFP::lgg-1 + rol-6(su1006)]; aak-2(ok524))* young adult worms. These worms are defective for α subunit of AMPK/AAK-2. In both studies, water was used as control and incubation at 37ºC for 1 hour as positive control. The statistical analysis was carried out using ANOVA with Turkey correction for multiple comparisons, from 3 independent experiments of at least 10 worms for each condition. Error bars show the standard error of the mean. n.s.: non-significant (*p*-value ≥ 0.05); ***: *p*-value < 0.001; *: *p*-value <0.05.

4.4. The treatment with metformin and salicylate does not induce significant changes in the expression of genes involved in autophagy.

Since a clear increase of autophagy was observed in LGG1::GFP worms treated with synergy, it was relevant to study a possible rise in the expression of genes related to autophagy in *C. elegans. The genes lgg-1, atg-9, atg-18 and sqst-1* were studied by means of RT-qPCR. TaqMan probes were designed to know the expression of these genes, and the relative expression was calculated by normalization with an endogenous gene (*pmp-3*), whose expression is stable regardless of conditions and genotype. The RT-qPCR was carried out from RNA of 2 strains: 40Q and 40Q;*aak2(ok524) rmIs133[unc-54p::40Q::YFP]-X* and *rmIs133[unc-54p::40Q::YFP ; aak-2(ok524]-X*, both untreated and treated with synergy, as seen in figure 4.6.

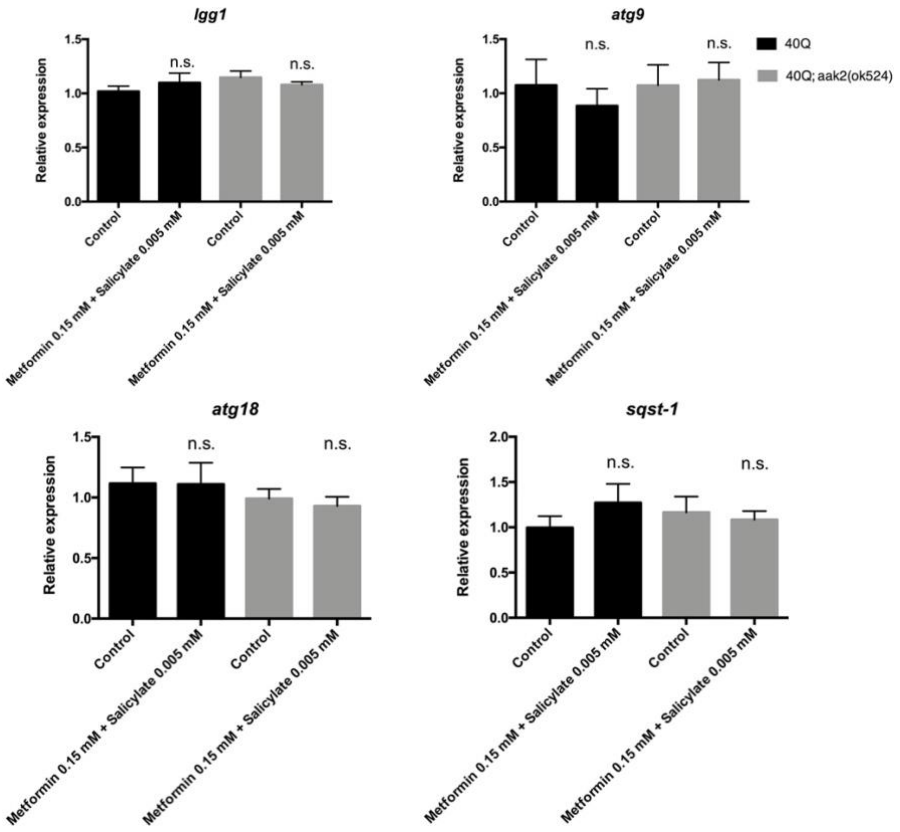

Figure 4.6. Relative expression of *lgg-1, atg-9, atg-18 and sqst-1.* In the strain 40Q (*rmIs133[unc- 54p::40Q::YFP]-X*) and the same strain defective for *aak-2* (*rmIs133[unc-54p::40Q::YFP ; aak-2(ok524) X*), after treatment with synergy. Water was used as control. Gene expression was normalized to an endogenous gene, pmp-3. The statistical analysis was carried out using ANOVA with Turkey correction for multiple comparisons, in 5 populations and 3 biological replicates for each condition. Error bars show the standard error of the mean. n.s.: non-significant (p-value ≥ 0.05).

4.5. Study of the involved AMPK downstream effectors in the response to metformin and salicylate

Different AMPK-activated transcription factors were studied to investigate their involvement in the mechanism set off by metformin and salicylate, since it remains unclear whether the alleviation is exclusively dependent on AMPK, or other signaling pathways are implicated, since both drugs act pleiotropically.

In the case of HLH-30, HLH-30::GFP worms were treated with 2mM metformin and with synergy. Worms were categorized as cytoplasmic (non-visible translocation), weak nuclear (only visible translocation in tail) and strong nuclear (visible translocation in tail and head). As a positive control, animals were incubated at 37°C for 1 hour. As seen in figure 4.7, there was no HLH-30 translocation and its subcellular localization was cytoplasmatic in all treated worms.

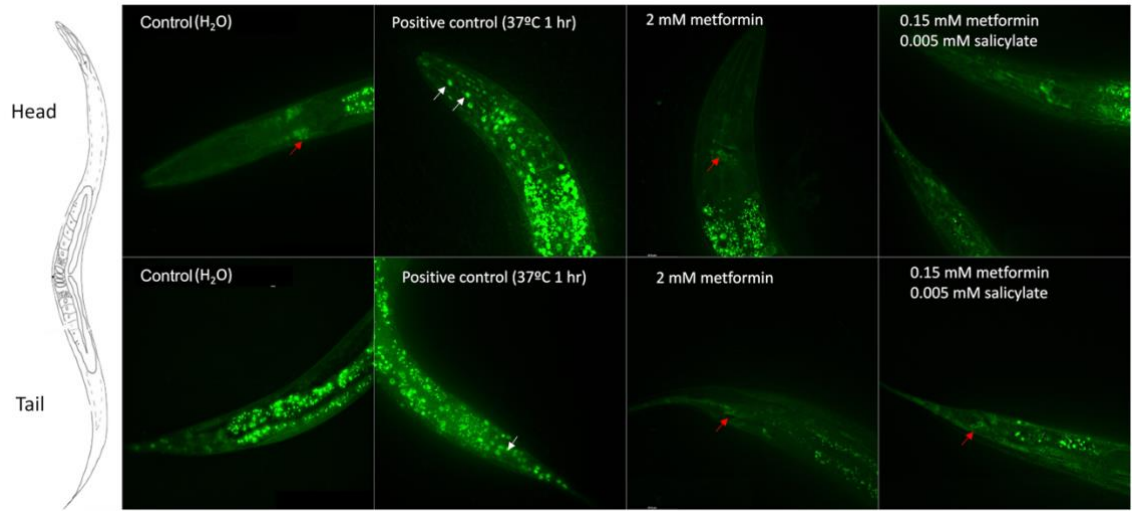

Figure 4.7. Representative images of head and tail of HLH-30::GFP young adult worms. Worms were cultured in 2mM metformin and with synergy. Incubation at 37ºC for 1 hour and water were used as positive and negative controls, respectively. Red arrows indicate the localization of HLH-30 in the cytoplasm when treated and white arrows indicate its localization in the nucleus when incubated at 37 ºC. Images were taken using a Leica DM6 B fluorescence microscope at 63x and with an exposure of 100 ms. Brightness and contrast values were modified with Fiji software for visualization purposes.

For the study of SKN-1, SKN-1::GFP worms were treated with 2mM metformin and with synergy. As a positive control, animals were incubated with 7.5 mM H_2O_2 for an hour to promote nuclear entry of SKN-1. As seen in figure 4.8, the was no SKN-1 translocation to the nucleus after treatment.

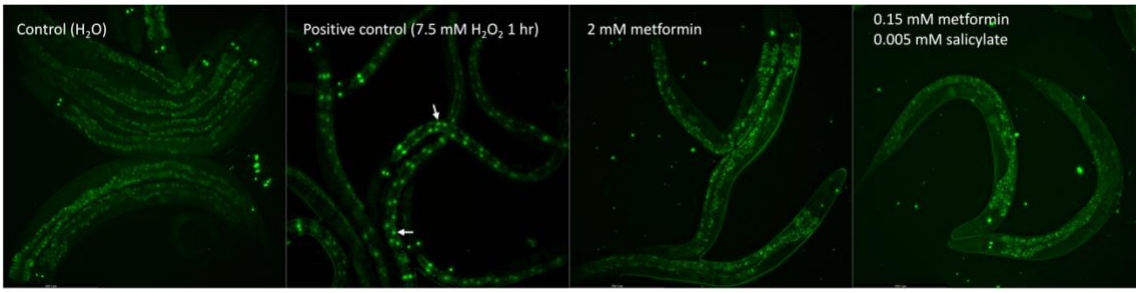

Figure 4.8. Representative images of SKN-1::GFP young adult worms. Worms were cultured in 2mM metformin and with synergy. Incubation with 7.5 mM H_2O_2 for 1 hour and water were used as positive and negative controls, respectively. White arrows indicate the translocated SKN-1 in the intestine nuclei. SKN-1 is always expressed in ASI neurons, and they are indicated by blue arrows. Images were taken using a Leica DM6 B fluorescence microscope at 20x and with an exposure of 100 ms. Brightness and contrast values were modified with Fiji software for visualization purposes.

Regarding DAF-16, TJ356 worms were treated with 2mM metformin and with synergy. As a positive control, animals were incubated at 37°C for 1 hour to induce translocation. As seen in figure 4.9, there was no DAF-16 translocation, and its subcellular localization was cytoplasmatic after treatment in all trials.

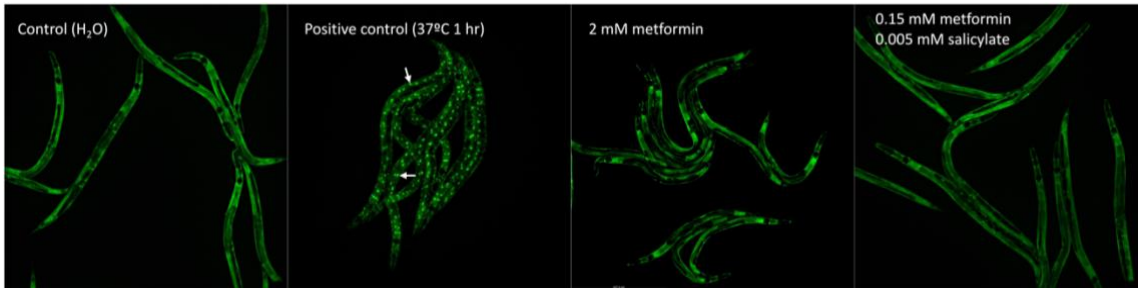

Figure 4.9. Representative images of DAF-16::GFP young adult worms. Worms were cultured in 2mM metformin and with synergy. Incubation at 37ºC for 1 hour and water were used as positive and negative controls, respectively. White arrows indicate nuclear accumulation of DAF-16 after incubation at 37 ºC. Images were taken using a Leica DM6 B fluorescence microscope at 10x and with an exposure of 100 ms. Brightness and contrast values were modified with Fiji software for visualization purposes.

One of the aims was to further study the effect of the transcription factor DAF-16 in the process triggered by the synergic effect of metformin and salicylate to protect from polyQ toxicity. For this end, a RNA interference experiment was designed, feeding 40Q::YFP worms with *E. coli* HT115 transfected with the vector pL4440 including the *daf-16* insert and not including it (empty vector). These worms were then treated with metformin and salicylate.

In the worms fed with bacteria containing the empty vector, a usual rescue of polyQ aggregates provided by treatment was expected, and this would work as a control. Nevertheless, there was no significant difference between the treated and untreated worms eating bacteria with empty vector, nor in the worms eating bacteria with *daf-16* insert (figure 4.10).

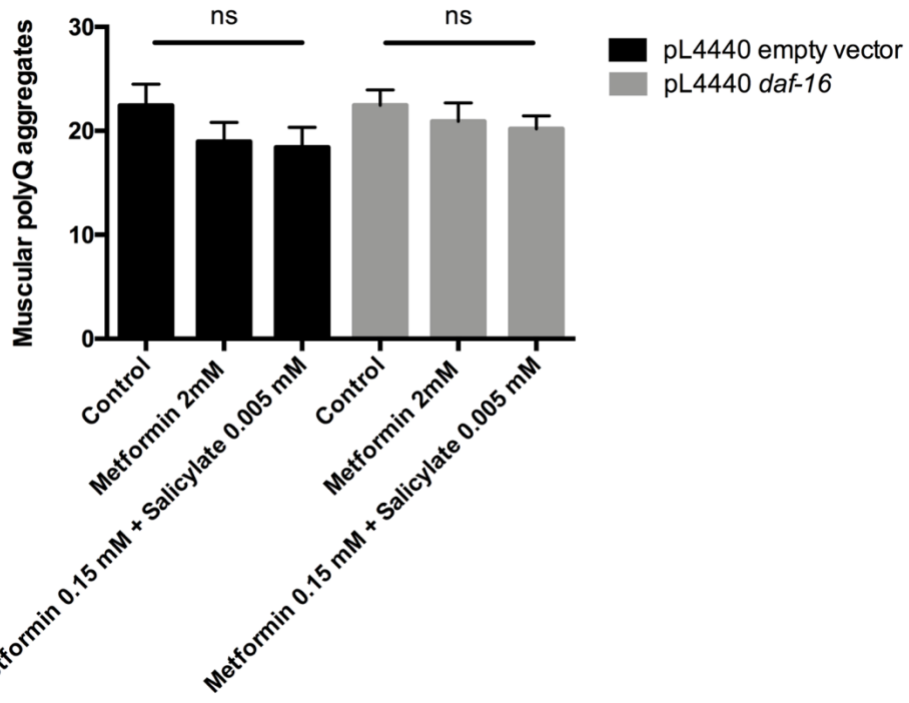

Figure 4.10. Variation in the average number of muscular polyQ aggregates in *rmIs133[unc-54p::40Q::YFP]-X in* young adult worms. These worms were fed with *E. coli* HT115 bacteria expressing the vector with daf-16 insert (grey) and expressing the empty vector (black). The strains were treated with synergy, 2 mM metformin and water were used as negative control. The statistical analysis was carried out using ANOVA with Turkey correction for multiple comparisons, from 3 repetitions of at least 10 samples for each condition. Error bars show the standard error of the mean. n.s.: non-significant (*p*-value ≥ 0,05).

5. Discussion

One of the aims of this project was to assess if the protection provided by the synergic effect of metformin and salicylate also worked in solid media, since the availability of these compounds in this type of media was unknown. As appreciated in figure 4.2, there was a significant reduction in the number of polyQ aggregates in worms treated with metformin and salicylate compared to untreated worms.

The significant difference is comparable to the previously obtained in liquid media (Gómez-Escribano et al., 2020). Therefore, the pharmacological efficacy of metformin and salicylate is preserved regardless of the type of media. This finding is relevant because worms cultured in liquid media are subjected to an additional stress which alters the results, since worms cultured in liquid media tend to show less aggregates. That is the reason we suggest that the experiments carried out in solid media better reflect the real effect of the synergic combination of metformin and salicylate. The results also display the importance of metformin and salicylate have a rescuing effect regardless of the administration via since *C. elegans* can take up compounds orally or through the cuticle (S. Giunti et al., 2021).

Moreover, this finding makes solid culture a proper alternative for pharmacological assays since plates are the standard practice in *C. elegans* maintenance. Solid media avoids having to use mandatorily a bleaching protocol to obtain a synchronized population because it is possible to add gravid hermaphrodites in the plates and remove them after they have laid the eggs. Therefore, pharmacological assays in solid media are very useful when using very sensitive strains that cannot tolerate bleaching.

Additionally, these results prove that the effect provided by synergy can reduce aggregates to the same level as higher doses of metformin (2 mM). Having the possibility of reducing the amount of the administered metformin and salicylate is extremely interesting for patients to avoid side effects since both drugs are pleiotropic. Currently, a clinical trial is being launched driven by the results obtained in the laboratory, to determine the effect of metformin in HD patients.

Another aim of this project was to study how AMPK activation rescued the polyQ aggregation phenotype and affected autophagy. Figure 4.3 displays the necessity of functional AMPK to reduce the neurotoxic effects of extended polyQs. The rescue in the 40Q strain is similar to the one observed in figure 4.2. However, the strain carrying *aak-2* loss of function had a significant increase in the number of muscular polyQ aggregates compared to the wildtype and the rescue provided by synergy was lost. Therefore, it can be confirmed in agreement with other results (Arnoux et al., 2018; Gómez-Escribano et al., 2020; Sanchis et al., 2019) that the rescue offered by the synergy depends on the catalytic subunit of AMPK.

We analyzed the potential increase in autophagy in both the *aak-2* defective strain and the wild-type strain when treated with a combination of metformin and salicylate. To deepen into the effect induced by synergy and how it can activate autophagy through AMPK (Lu et al., 2021; Ren et al., 2020), autophagy was measured in treated worms and in worms defective for the α subunit of AMPK. Autophagy can be indirectly measured by observing GFP-positive punctate areas in LGG1::GFP worms that indicate autophagosomal structures in hypodermal seam cells, as in Figure 4.4.

Figure 4.5 shows a significant increase in punctate areas worms treated with synergy, verifying that the protection provided by synergic effect acts through LGG-1 mediated autophagy. However, there is no significant difference in the number of punctate areas when treating 40Q;*aak-2(ok524)* worms with synergy. This suggests that the synergic effect provided by metformin and salicylate needs AMPK to activate autophagy.

However, it is notable that there is a significant difference between the negative and positive control in the worms defective for *aak-2*. This suggest that autophagy is happening when worms are exposed to heat stress, but it must be activated through other pathways other than AMPK. The other signaling pathways activating autophagy as an attempt to compensate the lack of functional AMPK may be mTOR or PI3K/AKT (Benito-Cuesta et al., 2021; Heras-Sandoval et al., 2014).

Moreover, the expression of different genes related to autophagy was analyzed to further understand the pathways set off by synergic activation of AMPK. Considering the known role of autophagy in reducing protein aggregation-induced toxicity (Park et al., 2020).

As it can be observed in figure 4.6, none of the analysis showed a significant difference between the conditions, either between water and treatment, nor between 40Q and 40Q;*aak2(ok524)* strains. Even though, 5 different populations were analyzed, the results obtained by qPCR in *C. elegans* are not always reliable or reproducible since numerous phenotypes and transcripts differ massively between individuals (Chauve et al., 2020). Such variation in gene expression affects worms in several ways, affecting things like mutation penetrance, survival, developmental timing, and fecundity (Casanueva et al., 2012; Raj et al., 2010).

Further study would be necessary to gain more accurate understanding of these results, such as a protein quantification by western blot. Moreover, results obtain by RTqPCR are not solid since only transcribed RNA is being analyzed, it cannot measure the final amount of functional protein. This means there could be more expression of a specific gene, but it does not imply more protein is being translated.

Moreover, in the specific case of the gene of *lgg-1*, it is thought to be constitutively expressed and translated, regardless of the conditions. However, under conditions such as AMPK activation by metformin and salicylate, autophagy is activated after processing of LGG-1. LGG-1 is processed by attaching phosphatidylethanolamine to the C-terminal, which is left exposed when LGG-1 precursors are broken down by proteases, and then is associated to the phagosomal membrane. SQST-1 interacts with LGG-1 and attracts poly-ubiquitylated substrates into the expanding autophagosome to achieve a phagosomal membrane elongation to create a closed autophagosome(Springhorn & Hoppe, 2019). Therefore, LGG-1 may be being processed and SQST-1 may be functioning, so autophagy may be happening, but it cannot be detected by qPCR.

All together, these results confirm that the reduction in polyQ toxicity after synergistic treatment with metformin and salicylate is dependent on the α subunit of AMPK and that the rescue provided by AMPK activation acts via autophagy. At the end, autophagy is a mechanism of protein clearance and the accumulation of protein aggregates that can disrupt the autophagic flux is a common trait in several neurodegenerative diseases. Several studies have also confirmed that the upregulation of autophagy helps reducing the toxicity caused by polyQ aggregates in Huntington's disease (Jia et al., 2007; Ravikumar, 2002; Sarkar et al., 2007).

Moreover, to study the subcellular localization of different AMPK effectors, three different strains containing the transcription factors HLH-30, SKN-1 and DAF-16 linked to GFP were cultured in distinct conditions, as described in figures 4.7, 4.8 and 4.9. These figures show that the subcellular localization of all transcription factors is 100% cytoplasmatic after synergic treatment, hence there is no nuclear translocation of any of the factors when AMPK is activated. However, beneficial effects of AMPK activation exerted through DAF-16 have been described with no translocation of it (Greer et al., 2007b). Therefore, it is not possible to assume that these three transcription factors are not involved in the response triggered by synergic activation of AMPK.

Nonetheless, it is interesting to study the potential translocation of these transcription factors in other stages besides young adult.

Given the previous results, it was interesting to study more deeply the role of the transcription factor DAF-16 in the response triggered by the synergic activation of AMPK. In the RNAi experiment, the treated worms eating bacteria with the empty vector, were expected to display a rescue that was not seen, as shown in figure 4.10. There was not a reduction in polyQ aggregates similar to the same strain eating the usual bacteria. Therefore, the results of the RNAi experiment cannot be taken into account since the control did not work.

The lack of significant difference in the assay may be due to several reasons. One of them is the *E. coli* strain used to feed the worms in RNAi assay. The strain HT115 alters the basal polyQ aggregation pattern because some of its metabolites, such as GABA, are identified as protectors against neuronal degeneration (Urrutia et al., 2020). Therefore, the worms express fewer polyQ aggregates which do not show enough difference to be significant nor see the effect of the treatment.

A possible solution is to let the worms feed from the usual *E. coli* OP50 and, once they reach L2 stage, transfer them to the HT115 bacteria carrying the vector. So the silencing of *daf-16* does not occur since the beginning and probably the polyQ aggregation differences can be better appreciated.

Finally, further research is needed to clarify pathways involved in the alleviation of polyQ induced toxicity by metformin and salicylate and analyze how the loss of function of aak-2 can affect the subcellular location of HLH-30, SKN-1 and DAF-16 after treatment.

6. Conclusions

The project carried out leads to the following conclusions:

1. The synergic effect of metformin and salicylate reduces polyQ toxicity in solid media in an AMPK-dependent manner.
2. Synergistic treatment with metformin and salicylate is inducing the autophagic flux, possibly increasing removal of polyQ aggregates.
3. Autophagy activation by the synergic effect of metformin and salicylate is dependent of AMPK.
4. Additional experiments are necessary to exclude the involvement of downstream AMPK effectors in the reduction of polyglutamine aggregation with metformin and salicylate treatment.

7. Bibliography

ALTUN, Z. F., CHEN, B., WANG, Z.-W., & HALL, D. H. (2009). High resolution map of *Caenorhabditis elegans* gap junction proteins. *Developmental Dynamics*, *238*(8), 1936–1950. https://doi.org/10.1002/dvdy.22025

AN, J. H., & BLACKWELL, T. K. (2003). SKN-1 links *C. elegans* mesendodermal specification to a conserved oxidative stress response. *Genes & Development*, *17*(15), 1882–1893. https://doi.org/10.1101/gad.1107803

ARNOUX, I., WILLAM, M., GRIESCHE, N., KRUMMEICH, J., WATARI, H., OFFERMANN, N., WEBER, S., NARAYAN DEY, P., CHEN, C., MONTEIRO, O., BUETTNER, S., MEYER, K., BANO, D., RADYUSHKIN, K., LANGSTON, R., LAMBERT, J. J., WANKER, E., METHNER, A., KRAUSS, S., … STROH, A. (2018). Metformin reverses early cortical network dysfunction and behavior changes in Huntington's disease. *ELife*, *7*. https://doi.org/10.7554/eLife.38744

AVILA, D., HELMCKE, K., & ASCHNER, M. (2012). The *Caenorhabiditis elegans* model as a reliable tool in neurotoxicology. *Human & Experimental Toxicology*, *31*(3), 236–243. https://doi.org/10.1177/0960327110392084

BARNES, K., INGRAM, J. C., PORRAS, O. H., BARROS, L. F., HUDSON, E. R., FRYER, L. G. D., FOUFELLE, F., CARLING, D., HARDIE, D. G., & BALDWIN, S. A. (2002). Activation of GLUT1 by metabolic and osmotic stress: potential involvement of AMP-activated protein kinase (AMPK). *Journal of Cell Science*, *115*(11), 2433–2442. https://doi.org/10.1242/jcs.115.11.2433

BAYLIS, H. A., & VÁZQUEZ-MANRIQUE, R. P. (2012). Genetic analysis of IP3 and calcium signalling pathways in C. elegans. *Biochimica et Biophysica Acta (BBA) - General Subjects*, *1820*(8), 1253–1268. https://doi.org/10.1016/j.bbagen.2011.11.009

BENITO-CUESTA, I., ORDÓÑEZ-GUTIÉRREZ, L., & WANDOSELL, F. (2021). AMPK activation does not enhance autophagy in neurons in contrast to MTORC1 inhibition: different impact on β-amyloid clearance. *Autophagy*, *17*(3), 656–671. https://doi.org/10.1080/15548627.2020.1728095

BISHOP, N. A., & GUARENTE, L. (2007). Two neurons mediate diet-restriction-induced longevity in C. elegans. *Nature*, *447*(7144), 545–549. https://doi.org/10.1038/nature05904

BOHANNA, I., GEORGIOU-KARISTIANIS, N., SRITHARAN, A., ASADI, H., JOHNSTON, L., CHURCHYARD, A., & EGAN, G. (2011). Diffusion Tensor Imaging in Huntington's disease reveals distinct patterns of white matter degeneration associated with motor and cognitive deficits. *Brain Imaging and Behavior*, *5*(3), 171–180. https://doi.org/10.1007/s11682-011-9121-8

BRAY, G. A., EDELSTEIN, S. L., CRANDALL, J. P., ARODA, V. R., FRANKS, P. W., FUJIMOTO, W., & HORTON, E. (2012). Long-Term Safety, Tolerability, and Weight Loss Associated With Metformin in the Diabetes Prevention Program Outcomes Study. *Diabetes Care*, *35*(4), 731–737. https://doi.org/10.2337/dc11-1299

BRENNER, S. (1974). THE GENETICS OF *CAENORHABDITIS ELEGANS*. *Genetics*, *77*(1), 71–94. https://doi.org/10.1093/genetics/77.1.71

C. elegans Sequencing Consortium. (1998). Genome Sequence of the Nematode *C. elegans* : A Platform for Investigating Biology. *Science*, *282*(5396), 2012–2018. https://doi.org/10.1126/science.282.5396.2012

CASANUEVA, M. O., BURGA, A., & LEHNER, B. (2012). Fitness Trade-Offs and Environmentally Induced Mutation Buffering in Isogenic *C. elegans*. *Science*, *335*(6064), 82–85. https://doi.org/10.1126/science.1213491

CHAUVE, L., LE PEN, J., HODGE, F., TODTENHAUPT, P., BIGGINS, L., MISKA, E. A., ANDREWS, S., & CASANUEVA, O. (2020). High-Throughput Quantitative RT-PCR in Single and Bulk C. elegans Samples Using Nanofluidic Technology. *Journal of Visualized Experiments*, *159*. https://doi.org/10.3791/61132

CONDELLO, M., PELLEGRINI, E., CARAGLIA, M., & MESCHINI, S. (2019). Targeting Autophagy to Overcome Human Diseases. *International Journal of Molecular Sciences*, *20*(3), 725. https://doi.org/10.3390/ijms20030725

CORK, G. K., THOMPSON, J., & SLAWSON, C. (2018). Real Talk: The Inter-play Between the mTOR, AMPK, and Hexosamine Biosynthetic Pathways in Cell Signaling. *Frontiers in Endocrinology*, *9*. https://doi.org/10.3389/fendo.2018.00522

COSTA, M. D., & MACIEL, P. (2022). Modifier pathways in polyglutamine (PolyQ) diseases: from genetic screens to drug targets. *Cellular and Molecular Life Sciences*, *79*(5), 274. https://doi.org/10.1007/s00018-022-04280-8

COX, D., RAEBURN, C., SUI, X., & HATTERS, D. M. (2020). Protein aggregation in cell biology: An aggregomics perspective of health and disease. *Seminars in Cell & Developmental Biology*, *99*, 40–54. https://doi.org/10.1016/j.semcdb.2018.05.003

DICKINSON, D. J., & GOLDSTEIN, B. (2016). CRISPR-Based Methods for *Caenorhabditis elegans* Genome Engineering. *Genetics*, *202*(3), 885–901. https://doi.org/10.1534/genetics.115.182162

FAN, H.-C., HO, L.-I., CHI, C.-S., CHEN, S.-J., PENG, G.-S., CHAN, T.-M., LIN, S.-Z., & HARN, H.-J. (2014). Polyglutamine (PolyQ) Diseases: Genetics to Treatments. *Cell Transplantation*, *23*(4–5), 441–458. https://doi.org/10.3727/096368914X678454

FIELENBACH, N., & ANTEBI, A. (2008). *C. elegans* dauer formation and the molecular basis of plasticity. *Genes & Development*, *22*(16), 2149–2165. https://doi.org/10.1101/gad.1701508

FIRE, A., XU, S., MONTGOMERY, M. K., KOSTAS, S. A., DRIVER, S. E., & MELLO, C. C. (1998). Potent and specific genetic interference by double-stranded RNA in Caenorhabditis elegans. *Nature*, *391*(6669), 806–811. https://doi.org/10.1038/35888

FRANCO-JUÁREZ, B., GÓMEZ-MANZO, S., HERNÁNDEZ-OCHOA, B., CÁRDENAS-RODRÍGUEZ, N., ARREGUIN-ESPINOSA, R., PÉREZ DE LA CRUZ, V., & ORTEGA-CUELLAR, D. (2021). Effects of High Dietary Carbohydrate and Lipid Intake on the Lifespan of C. elegans. *Cells*, *10*(9), 2359. https://doi.org/10.3390/cells10092359

G. VONSATTEL, J. P., & DIFIGLIA, M. (1998). Huntington Disease. *Journal of Neuropathology and Experimental Neurology*, *57*(5), 369–384. https://doi.org/10.1097/00005072-199805000-00001

GHOSH, R., & TABRIZI, S. J. (2018). *Clinical Features of Huntington's Disease* (pp. 1–28). https://doi.org/10.1007/978-3-319-71779-1_1

GIUNTI, P. (1998). The role of the SCA2 trinucleotide repeat expansion in 89 autosomal dominant cerebellar ataxia families. Frequency, clinical and genetic correlates. *Brain*, *121*(3), 459–467. https://doi.org/10.1093/brain/121.3.459

GIUNTI, S., ANDERSEN, N., RAYES, D., & DE ROSA, M. J. (2021). Drug discovery: Insights from the invertebrate *Caenorhabditis elegans*. *Pharmacology Research & Perspectives*, *9*(2). https://doi.org/10.1002/prp2.721

GÓMEZ-ESCRIBANO, A. P., BONO-YAGÜE, J., GARCÍA-GIMENO, M. A., SEQUEDO, M. D., HERVÁS, D., FORNÉS-FERRER, V., TORRES-SÁNCHEZ, S. C., MILLÁN, J. M., SANZ, P., & VÁZQUEZ-MANRIQUE, R. P. (2020). Synergistic activation of AMPK prevents from polyglutamine-induced toxicity in Caenorhabditis elegans. *Pharmacological Research*, *161*. https://doi.org/10.1016/j.phrs.2020.105105

GREER, E. L., DOWLATSHAHI, D., BANKO, M. R., VILLEN, J., HOANG, K., BLANCHARD, D., GYGI, S. P., & BRUNET, A. (2007a). An AMPK-FOXO Pathway Mediates Longevity Induced by a Novel Method of Dietary Restriction in C. elegans. *Current Biology*, *17*(19), 1646–1656. https://doi.org/10.1016/j.cub.2007.08.047

HAWLEY, S. A., FULLERTON, M. D., ROSS, F. A., SCHERTZER, J. D., CHEVTZOFF, C., WALKER, K. J., PEGGIE, M. W., ZIBROVA, D., GREEN, K. A., MUSTARD, K. J., KEMP, B. E., SAKAMOTO, K., STEINBERG, G. R., & HARDIE, D. G. (2012). The Ancient Drug Salicylate Directly Activates AMP-Activated Protein Kinase. *Science*, *336*(6083), 918–922. https://doi.org/10.1126/science.1215327

HERAS-SANDOVAL, D., PÉREZ-ROJAS, J. M., HERNÁNDEZ-DAMIÁN, J., & PEDRAZA-CHAVERRI, J. (2014). The role of PI3K/AKT/mTOR pathway in the modulation of autophagy and the clearance of protein aggregates in neurodegeneration. *Cellular Signalling*, *26*(12), 2694–2701. https://doi.org/10.1016/j.cellsig.2014.08.019

HERVÁS, D., FORNÉS-FERRER, V., GÓMEZ-ESCRIBANO, A. P., SEQUEDO, M. D., PEIRÓ, C., MILLÁN, J. M., & VÁZQUEZ-MANRIQUE, R. P. (2017). Metformin intake associates with better cognitive function in patients with Huntington's disease. *PLOS ONE*, *12*(6), e0179283. https://doi.org/10.1371/journal.pone.0179283

HESP, K., SMANT, G., & KAMMENGA, J. E. (2015). Caenorhabditis elegans DAF-16/FOXO transcription factor and its mammalian homologs associate with age-related disease. *Experimental Gerontology*, *72*, 1–7. https://doi.org/10.1016/j.exger.2015.09.006

HUANG, E. S., STRATE, L. L., HO, W. W., LEE, S. S., & CHAN, A. T. (2011). Long-Term Use of Aspirin and the Risk of Gastrointestinal Bleeding. *The American Journal of Medicine*, *124*(5), 426–433. https://doi.org/10.1016/j.amjmed.2010.12.022

HWANG, M., SHRESTHA, C., KANG, S., & KIM, J. (2022). MEKK-3 Acts Cooperatively with NSY-1 in SKN-1-Dependent Manner against Oxidative Stress and Aging in Caenorhabditis elegans. *Biology*, *11*(10), 1526. https://doi.org/10.3390/biology11101526

J G WHITE, E SOUTHGATE, J N THOMSON, & S BRENNER. (1986). The structure of the nervous system of the nematode *Caenorhabditis elegans*. *Philosophical Transactions of the Royal Society of London. B, Biological Sciences*, *314*(1165), 1–340. https://doi.org/10.1098/rstb.1986.0056

JIA, K., HART, A. C., & LEVINE, B. (2007). Autophagy Genes Protect Against Disease Caused by Polyglutamine Expansion Proteins in *Caenorhabditis elegans*. *Autophagy*, *3*(1), 21–25. https://doi.org/10.4161/auto.3528

KIM, J., YANG, G., KIM, Y., KIM, J., & HA, J. (2016). AMPK activators: mechanisms of action and physiological activities. *Experimental & Molecular Medicine*, *48*(4), e224–e224. https://doi.org/10.1038/emm.2016.16

KLIONSKY, D. J., ABELIOVICH, H., AGOSTINIS, P., AGRAWAL, D. K., ALIEV, G., ASKEW, D. S., BABA, M., BAEHRECKE, E. H., BAHR, B. A., BALLABIO, A., BAMBER, B. A., BASSHAM, D. C., BERGAMINI, E., BI, X., BIARD-PIECHACZYK, M., BLUM, J. S., BREDESEN, D. E., BRODSKY, J. L., BRUMELL, J. H., … DETER, R. L. (2008). Guidelines for the use and interpretation of assays for monitoring autophagy in higher eukaryotes. *Autophagy*, *4*(2), 151–175. https://doi.org/10.4161/auto.5338

KUMSTA, C., CHANG, J. T., LEE, R., TAN, E. P., YANG, Y., LOUREIRO, R., CHOY, E. H., LIM, S. H. Y., SAEZ, I., SPRINGHORN, A., HOPPE, T., VILCHEZ, D., & HANSEN, M. (2019). The autophagy receptor p62/SQST-1 promotes proteostasis and longevity in C. elegans by inducing autophagy. *Nature Communications*, *10*(1), 5648. https://doi.org/10.1038/s41467-019-13540-4

LAPIERRE, L. R., DE MAGALHAES FILHO, C. D., MCQUARY, P. R., CHU, C.-C., VISVIKIS, O., CHANG, J. T., GELINO, S., ONG, B., DAVIS, A. E., IRAZOQUI, J. E., DILLIN, A., & HANSEN, M. (2013). The TFEB orthologue HLH-30 regulates autophagy and modulates longevity in Caenorhabditis elegans. *Nature Communications*, *4*(1), 2267. https://doi.org/10.1038/ncomms3267

LEVINE, B., & KROEMER, G. (2019). Biological Functions of Autophagy Genes: A Disease Perspective. *Cell*, *176*(1–2), 11–42. https://doi.org/10.1016/j.cell.2018.09.048

LI, Q., HARVEY, L. M., & MCNEIL, B. (2009). Oxidative stress in industrial fungi. *Critical Reviews in Biotechnology*, *29*(3), 199–213. https://doi.org/10.1080/07388550903004795

LIN, X.-X., SEN, I., JANSSENS, G. E., ZHOU, X., FONSLOW, B. R., EDGAR, D., STROUSTRUP, N., SWOBODA, P., YATES, J. R., RUVKUN, G., & RIEDEL, C. G. (2018). DAF-16/FOXO and HLH-30/TFEB function as combinatorial transcription factors to promote stress resistance and longevity. *Nature Communications*, *9*(1), 4400. https://doi.org/10.1038/s41467-018-06624-0

LU, G., WU, Z., SHANG, J., XIE, Z., CHEN, C., & ZHANG, C. (2021). The effects of metformin on autophagy. *Biomedicine & Pharmacotherapy*, *137*, 111286. https://doi.org/10.1016/j.biopha.2021.111286

MACIEL, P., GASPAR, C., DESTEFANO, A. L., SILVEIRA, I., COUTINHO, P., RADVANY, J., DAWSON, D. M., SUDARSKY, L., GUIMARIES, J., LOUREIRO, J. E. L., NEZARATI,', M. M., CORWIN,'', L. 1, LOPES-CENDES, I., ROOKE, K., ROSENBERG,', R., MACLEOD, P., FARRER, L. A., SEQUEIROS, J., & ROULEAU', G. A. (1995). Correlation between CAG Repeat Length and Clinical Features in Machado-Joseph Disease. In *Am. J. Hum. Genet* (Vol. 57).

MARTINA, J. A., CHEN, Y., GUCEK, M., & PUERTOLLANO, R. (2012). MTORC1 functions as a transcriptional regulator of autophagy by preventing nuclear transport of TFEB. *Autophagy*, *8*(6), 903–914. https://doi.org/10.4161/auto.19653

MARTINEZ-VICENTE, M., TALLOCZY, Z., WONG, E., TANG, G., KOGA, H., KAUSHIK, S., DE VRIES, R., ARIAS, E., HARRIS, S., SULZER, D., & CUERVO, A. M. (2010). Cargo recognition failure is responsible for inefficient autophagy in Huntington's disease. *Nature Neuroscience*, *13*(5), 567–576. https://doi.org/10.1038/nn.2528

MORLEY, J. F., BRIGNULL, H. R., WEYERS, J. J., & MORIMOTO, R. I. (2002). The threshold for polyglutamine-expansion protein aggregation and cellular toxicity is dynamic and influenced by aging in *Caenorhabditis elegans*. *Proceedings of the National Academy of Sciences*, *99*(16), 10417–10422. https://doi.org/10.1073/pnas.152161099

MUÑOZ-LOBATO, F., RODRÍGUEZ-PALERO, M. J., NARANJO-GALINDO, F. J., SHEPHARD, F., GAFFNEY, C. J., SZEWCZYK, N. J., HAMAMICHI, S., CALDWELL, K. A., CALDWELL, G. A., LINK, C. D., & MIRANDA-VIZUETE, A. (2014). Protective Role of DNJ-27/ERdj5 in *Caenorhabditis elegans* Models of Human Neurodegenerative Diseases. *Antioxidants & Redox Signaling*, *20*(2), 217–235. https://doi.org/10.1089/ars.2012.5051

MUSCHIOL, D., SCHROEDER, F., & TRAUNSPURGER, W. (2009). Life cycle and population growth rate of Caenorhabditis elegans studied by a new method. *BMC Ecology*, *9*(1), 14. https://doi.org/10.1186/1472-6785-9-14

MUSI, N., HIRSHMAN, M. F., NYGREN, J., SVANFELDT, M., BAVENHOLM, P., ROOYACKERS, O., ZHOU, G., WILLIAMSON, J. M., LJUNQVIST, O., EFENDIC, S., MOLLER, D. E., THORELL, A., & GOODYEAR, L. J. (2002). Metformin Increases AMP-Activated Protein Kinase Activity in Skeletal Muscle of Subjects With Type 2 Diabetes. *Diabetes*, *51*(7), 2074–2081. https://doi.org/10.2337/diabetes.51.7.2074

OGG, S., PARADIS, S., GOTTLIEB, S., PATTERSON, G. I., LEE, L., TISSENBAUM, H. A., & RUVKUN, G. (1997). The Fork head transcription factor DAF-16 transduces insulin-like metabolic and longevity signals in C. elegans. *Nature*, *389*(6654), 994–999. https://doi.org/10.1038/40194

ONKEN, B., & DRISCOLL, M. (2010). Metformin Induces a Dietary Restriction–Like State and the Oxidative Stress Response to Extend C. elegans Healthspan via AMPK, LKB1, and SKN-1. *PLoS ONE*, *5*(1), e8758. https://doi.org/10.1371/journal.pone.0008758

PARK, H., KANG, J.-H., & LEE, S. (2020). Autophagy in Neurodegenerative Diseases: A Hunter for Aggregates. *International Journal of Molecular Sciences*, *21*(9), 3369. https://doi.org/10.3390/ijms21093369

RAJ, A., RIFKIN, S. A., ANDERSEN, E., & VAN OUDENAARDEN, A. (2010). Variability in gene expression underlies incomplete penetrance. *Nature*, *463*(7283), 913–918. https://doi.org/10.1038/nature08781

RAVIKUMAR, B. (2002). Aggregate-prone proteins with polyglutamine and polyalanine expansions are degraded by autophagy. *Human Molecular Genetics*, *11*(9), 1107–1117. https://doi.org/10.1093/hmg/11.9.1107

REN, H., SHAO, Y., WU, C., MA, X., LV, C., & WANG, Q. (2020). Metformin alleviates oxidative stress and enhances autophagy in diabetic kidney disease via AMPK/SIRT1-FoxO1 pathway. *Molecular and Cellular Endocrinology*, *500*, 110628. https://doi.org/10.1016/j.mce.2019.110628

ROBIDA-STUBBS, S., GLOVER-CUTTER, K., LAMMING, D. W., MIZUNUMA, M., NARASIMHAN, S. D., NEUMANN-HAEFELIN, E., SABATINI, D. M., & BLACKWELL, T. K. (2012). TOR Signaling and Rapamycin Influence Longevity by Regulating SKN-1/Nrf and DAF-16/FoxO. *Cell Metabolism*, *15*(5), 713–724. https://doi.org/10.1016/j.cmet.2012.04.007

ROJAS, L. B. A., & GOMES, M. B. (2013). Metformin: an old but still the best treatment for type 2 diabetes. *Diabetology & Metabolic Syndrome*, *5*(1), 6. https://doi.org/10.1186/1758-5996-5-6

ROSS, C. A., & POIRIER, M. A. (2004). Protein aggregation and neurodegenerative disease. *Nature Medicine*, *10*(S7), S10–S17. https://doi.org/10.1038/nm1066

SALMINEN, A., & KAARNIRANTA, K. (2012). AMP-activated protein kinase (AMPK) controls the aging process via an integrated signaling network. *Ageing Research Reviews*, *11*(2), 230–241. https://doi.org/10.1016/j.arr.2011.12.005

SANCHIS, A., GARCÍA-GIMENO, M. A., CAÑADA-MARTÍNEZ, A. J., SEQUEDO, M. D., MILLÁN, J. M., SANZ, P., & VÁZQUEZ-MANRIQUE, R. P. (2019). Metformin treatment reduces motor and neuropsychiatric phenotypes in the zQ175 mouse model of Huntington disease. *Experimental & Molecular Medicine*, *51*(6), 1–16. https://doi.org/10.1038/s12276-019-0264-9

SARKAR, S., DAVIES, J. E., HUANG, Z., TUNNACLIFFE, A., & RUBINSZTEIN, D. C. (2007). Trehalose, a Novel mTOR-independent Autophagy Enhancer, Accelerates the Clearance of Mutant Huntingtin and α-Synuclein. *Journal of Biological Chemistry*, *282*(8), 5641–5652. https://doi.org/10.1074/jbc.M609532200

SCHINDELIN, J., ARGANDA-CARRERAS, I., FRISE, E., KAYNIG, V., LONGAIR, M., PIETZSCH, T., PREIBISCH, S., RUEDEN, C., SAALFELD, S., SCHMID, B., TINEVEZ, J.-Y., WHITE, D. J., HARTENSTEIN, V., ELICEIRI, K., TOMANCAK, P., & CARDONA, A. (2012). Fiji: an open-source platform for biological-image analysis. *Nature Methods*, *9*(7), 676–682. https://doi.org/10.1038/nmeth.2019

SPRINGHORN, A., & HOPPE, T. (2019). *Western blot analysis of the autophagosomal membrane protein LGG-1/LC3 in Caenorhabditis elegans* (pp. 319–336). https://doi.org/10.1016/bs.mie.2018.12.034

STEINBERG, G. R., DANDAPANI, M., & HARDIE, D. G. (2013). AMPK: mediating the metabolic effects of salicylate-based drugs? *Trends in Endocrinology & Metabolism*, *24*(10), 481–487. https://doi.org/10.1016/j.tem.2013.06.002

STRANGE, K. (2006). An Overview of C. elegan Biology: Methods and Applications. In *C. elegans* (pp. 1–11). Humana Press. https://doi.org/10.1385/1-59745-151-7:1

SULSTON, J. E., SCHIERENBERG, E., WHITE, J. G., & THOMSON, J. N. (1983). The embryonic cell lineage of the nematode Caenorhabditis elegans. *Developmental Biology*, *100*(1), 64–119. https://doi.org/10.1016/0012-1606(83)90201-4

TAKEUCHI, T., & NAGAI, Y. (2017). Protein Misfolding and Aggregation as a Therapeutic Target for Polyglutamine Diseases. *Brain Sciences*, *7*(12), 128. https://doi.org/10.3390/brainsci7100128

TANIDA, I., UENO, T., & KOMINAMI, E. (2008). *LC3 and Autophagy* (pp. 77–88). https://doi.org/10.1007/978-1-59745-157-4_4

TIMMONS, L., COURT, D. L., & FIRE, A. (2001). Ingestion of bacterially expressed dsRNAs can produce specific and potent genetic interference in Caenorhabditis elegans. *Gene*, *263*(1–2), 103–112. https://doi.org/10.1016/S0378-1119(00)00579-5

TRAN, H., BRUNET, A., GRENIER, J. M., DATTA, S. R., FORNACE, A. J., DISTEFANO, P. S., CHIANG, L. W., & GREENBERG, M. E. (2002). DNA Repair Pathway Stimulated by the Forkhead Transcription Factor FOXO3a Through the Gadd45 Protein. *Science*, *296*(5567), 530–534. https://doi.org/10.1126/science.1068712

TROTTIER, Y., BIANCALANA, V., & MANDEL, J. L. (1994). Instability of CAG repeats in Huntington's disease: relation to parental transmission and age of onset. *Journal of Medical Genetics*, *31*(5), 377–382. https://doi.org/10.1136/jmg.31.5.377

TRUJILLO-DEL RÍO, C., TORTAJADA-PÉREZ, J., GÓMEZ-ESCRIBANO, A. P., CASTERÁ, F., PEIRÓ, C., MILLÁN, J. M., HERRERO, M. J., & VÁZQUEZ-MANRIQUE, R. P. (2022). Metformin to treat Huntington disease: A pleiotropic drug against a multi-system disorder. In *Mechanisms of Ageing and Development* (Vol. 204). Elsevier Ireland Ltd. https://doi.org/10.1016/j.mad.2022.111670

URRUTIA, A., GARCÍA-ANGULO, V. A., FUENTES, A., CANEO, M., LEGÜE, M., URQUIZA, S., DELGADO, S. E., UGALDE, J., BURDISSO, P., & CALIXTO, A. (2020). Bacterially produced metabolites protect C. elegans neurons from degeneration. *PLOS Biology*, *18*(3), e3000638. https://doi.org/10.1371/journal.pbio.3000638

VÁZQUEZ-MANRIQUE, R. P., FARINA, F., CAMBON, K., DOLORES SEQUEDO, M., PARKER, A. J., MILLÁN, J. M., WEISS, A., DÉGLON, N., & NERI, C. (2016). AMPK activation protects from neuronal dysfunction and vulnerability across nematode, cellular and mouse models of Huntington's disease. *Human Molecular Genetics*, *25*(6), 1043–1058. https://doi.org/10.1093/hmg/ddv513

WORMATLAS, ALTUN, Z.F., HERNDON, L.A., WOLKOW, C.A., CROCKER, C., LINTS, R. AND HALL, D.H. (ed.s) 2002-2023. http://www.wormatlas.org

YAMAMOTO, A., CREMONA, M. L., & ROTHMAN, J. E. (2006). Autophagy-mediated clearance of huntingtin aggregates triggered by the insulin-signaling pathway. *Journal of Cell Biology*, *172*(5), 719–731. https://doi.org/10.1083/jcb.200510065

ZEČIĆ, A., & BRAECKMAN, B. P. (2020). DAF-16/FoxO in Caenorhabditis elegans and Its Role in Metabolic Remodeling. *Cells*, *9*(1), 109. https://doi.org/10.3390/cells9010109

ZHANG, H., CHANG, J. T., GUO, B., HANSEN, M., JIA, K., KOVÁ, A. L., KUMSTA, C., LAPIERRE, L. R., LEGOUIS, R., LIN, L., LU, Q., MELÉNDEZ, A., O'ROURKE, E. J., SATO, K., SATO, M., WANG, X., & WU, F. (2015). Guidelines for monitoring autophagy in Caenorhabditis elegans. In *Autophagy* (Vol. 11, Issue 1, pp. 9–27). Landes Bioscience. https://doi.org/10.1080/15548627.2014.1003478

UNIVERSITAT POLITÈCNICA DE VALÈNCIA

ANEXO I. RELACIÓN DEL TRABAJO CON LOS OBJETIVOS DE DESARROLLO SOSTENIBLE DE LA AGENDA 2030

Anexo al Trabajo de Fin de Grado y Trabajo de Fin de Máster: Relación del trabajo con los Objetivos de Desarrollo Sostenible de la agenda 2030.

Grado de relación del trabajo con los Objetivos de Desarrollo Sostenible (ODS).

Objetivos de Desarrollo Sostenibles	Alto	Medio	Bajo	No Procede
ODS 1. **Fin de la pobreza.**				x
ODS 2. **Hambre cero.**				x
ODS 3. **Salud y bienestar.**	x			
ODS 4. **Educación de calidad.**				x
ODS 5. **Igualdad de género.**				x
ODS 6. **Agua limpia y saneamiento.**				x
ODS 7. **Energía asequible y no contaminante.**				x
ODS 8. **Trabajo decente y crecimiento económico.**				x
ODS 9. **Industria, innovación e infraestructuras.**				x
ODS 10. **Reducción de las desigualdades**.				x
ODS 11. **Ciudades y comunidades sostenibles**.				x
ODS 12. **Producción y consumo responsables.**				x
ODS 13. **Acción por el clima.**				x
ODS 14. **Vida submarina.**				x
ODS 15. **Vida de ecosistemas terrestres.**				x
ODS 16. **Paz, justicia e instituciones sólidas.**				x
ODS 17. **Alianzas para lograr objetivos.**				x

Descripción de la alineación del TFG/TFM con los ODS con un grado de relación más alto.

***Utilice tantas páginas como sea necesario.

El Objetivo de Desarrollo Sostenible (ODS) número 3, "Salud y Bienestar", se relaciona con la investigación de las rutas afectadas y los efectores activados por el tratamiento con metformina y salicilato para curar la enfermedad de Huntington y otras enfermedades de poliglutaminas de la siguiente manera:

El ODS 3 tiene como objetivo garantizar una vida saludable y promover el bienestar para todos en todas las edades. Dentro de este objetivo, se busca prevenir y tratar enfermedades, así como promover la salud mental y el bienestar en general.

La enfermedad de Huntington y otras enfermedades de poliglutaminas son trastornos neurodegenerativos que afectan la función cerebral y tienen un impacto significativo en la calidad de vida de los pacientes. posibles enfoques terapéuticos para su cura.

Al relacionar estos dos aspectos, la investigación de las rutas afectadas y los efectores activados

Editor: Secretaria General / UPV · D.L.: V-5092-2006 · ISSN: 1887-2298 · www.upv.es/secgen

de vida de los pacientes. La investigación de las rutas afectadas y los efectores activados por el tratamiento con metformina y salicilato busca entender mejor estos trastornos y encontrar posibles enfoques terapéuticos para su cura.

Al relacionar estos dos aspectos, la investigación de las rutas afectadas y los efectores activados por el tratamiento con metformina y salicilato para curar la enfermedad de Huntington y otras enfermedades de poliglutaminas contribuye directamente al ODS 3 al buscar mejorar la salud y el bienestar de las personas afectadas por estos trastornos. Además, al avanzar en la comprensión y el tratamiento de estas enfermedades, también se promueve el conocimiento científico y se fomenta la colaboración entre diferentes sectores, lo cual es esencial para lograr un progreso sostenible en el campo de la salud y el bienestar.

Editor: Secretaria General / UPV · D.L.: V-5092-2006 · ISSN: 1887-2298 · www.upv.es/secgen